

# Investigating the dynamics of ring polymers with different internal topologies

A Thesis

submitted to

Indian Institute of Science Education and Research Pune  
in partial fulfillment of the requirements for the  
BS-MS Dual Degree Programme

by

Vaibhav Chaturvedi



Indian Institute of Science Education and Research Pune  
Dr. Homi Bhabha Road,  
Pashan, Pune 411008, INDIA.

May, 2024

Supervisor: Dr. Apratim Chatterji

© Vaibhav Chaturvedi 2024

All rights reserved

# Certificate

This is to certify that this dissertation entitled Investigating the dynamics of ring polymers with different internal topologies towards the partial fulfilment of the BS-MS dual degree programme at the Indian Institute of Science Education and Research, Pune represents study/work carried out by Vaibhav Chaturvedi at Indian Institute of Science Education and Research under the supervision of Dr. Apratim Chatterji, Associate Professor, Department of Physics, during the academic year 2023-2024.



Dr. Apratim Chatterji

Committee:

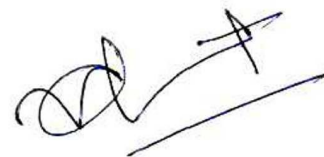
Dr. Apratim Chatterji

Dr. Shivprasad Patil



# Declaration

I hereby declare that the matter embodied in the report entitled Investigating the dynamics of ring polymers with different internal topologies are the results of the work carried out by me at the Department of Physics, Indian Institute of Science Education and Research, Pune, under the supervision of Dr. Apratim Chatterji and the same has not been submitted elsewhere for any other degree.

A handwritten signature in black ink, consisting of a series of loops and a long horizontal stroke at the end.

Vaibhav Chaturvedi



# Acknowledgments

First and foremost, I would like to thank my supervisor Dr. Apratim Chatterji for always having faith in me and guiding me through all of the problems that I faced in my work. I am extremely grateful for him always understanding my capabilities and giving me room to learn and work constructively while challenging me to grow and think critically as well. I am grateful to have gained a lot of invaluable insights and experience about research and academia from him. I would also like to thank the IISER Pune institute for not only giving me an opportunity to study and gain knowledge from here throughout my degree but also providing me the support and infrastructure to carry out my project work whether it is semester projects or MS thesis project. I would also like to thank Prof. Arijit Bhattacharyay as well for giving me an opportunity for a project with him. I would especially like to thank Dr. Shivprasad Patil as well for being my thesis expert and always supporting me fully and helping me despite me not even having any project with him. I thank both of them wholeheartedly for trusting me and my capabilities.

I would also like to thank my parents for always supporting me and believing in me. I am glad that my mumma and dad are always proud of me and everything that I am is because of them. My father has always been a great role-model to me and my mother has always been so supportive and loving.

I would also like to thank my close friends here at IISER Pune. They made life so much better and enjoyable here with so many memories and good times. Even my basketball buddies for so many exciting pick-up games in evenings and a great culture for the sport. In fact most of the sports friends. And I cannot forget to thank my lab-mates and friends in the lab. They have always been so supportive and fun to work and hangout with! I always felt like home and the work environment is so chill and comfortable with great discussions as well.





# Abstract

The aim of this thesis is to investigate relaxation times of different polymer segments in topologically modified ring polymeric systems. These topologically modified ring polymers are relevant in the context of bacterial chromosome organizations<sup>[5]</sup>. But it is expected that new emergent polymer physics phenomena will result as a consequence of the different topological modifications within ring polymers. In particular, in an already published paper in the soft matter group of Prof. Apratim Chatterji<sup>[4]</sup>, there are set of 12 different architectures that have already been designed to study the role of internal loops in organization of polymer segments within a confining cylinder. In addition, the group is also currently investigating the organization of polymer segments as a consequence of internal loops in spherical confinements. Due to the modified architecture, the dynamics (relaxation properties) of loops with respect to each other and thereby the entire polymeric system can be very different from what is known for ring or linear polymers. Single small loops repel other loops entropically and likely entangle less compared to linear polymeric systems. The relatively fast relaxation of internal loops could lead to a much faster relaxation in topologically modified ring polymers as compared to standard ring polymers. We have focused on four different architectures : Linear Chain, Ring, "Inverted-8"/Dumbbell and Arc2. We have shown results of how their size is affected due to introduction of the cross-links. Also, how their diffusion properties change and how the various conformation vectors within these polymers relax. We have also calculated the scaling through our data for these cases and compared it across these architectures.



# Contents

<b>Abstract</b>	<b>ix</b>
<b>1 Introduction</b>	<b>1</b>
1.1 Background of Soft Matter Physics . . . . .	1
1.2 Polymer Physics . . . . .	2
1.3 Why study various Polymer Architectures and their Relaxation properties? .	4
1.4 Thesis Outline . . . . .	5
<b>2 Theory and Methods</b>	<b>7</b>
2.1 Role of Computational Methods . . . . .	7
2.2 Bead-spring model . . . . .	8
2.3 Model Description . . . . .	10
2.4 Radius of Gyration ( $R_g$ ) . . . . .	13
2.5 Diffusion related analysis method . . . . .	13
2.6 Vector conformation relaxation analysis method . . . . .	15
2.7 Various Architectures Used . . . . .	17
<b>3 Radius of Gyration</b>	<b>27</b>
3.1 Comparing $R_g$ data across various architectures . . . . .	28

<b>4</b>	<b>Diffusion Scaling</b>	<b>31</b>
4.1	Comparison of Diffusion Constants (D) . . . . .	31
4.2	Comparison of Diffusion times ( $\tau_{diff}$ ) . . . . .	35
<b>5</b>	<b>Conformation Relaxation</b>	<b>39</b>
5.1	Analyzing and choosing the slowest relaxation times across various architectures	39
5.2	Comparison of $\tau_{conf}$ across various architectures . . . . .	43
<b>6</b>	<b>Conclusion and Future Direction</b>	<b>47</b>

# Chapter 1

## Introduction

### 1.1 Background of Soft Matter Physics

Soft Matter Physics essentially branches out of one of the fundamental fields in Physics, Condensed Matter Physics. Soft Matter Physics, as the name suggests, deals with the study of Soft Matter. What is Soft Matter? These are materials which exhibit intermediate properties between solid and liquid states of matter. We have a few examples such as Polymers, Colloids, Liquid Crystals, Foams etc. Everyday life examples can include semi-solid gels or paste, plastics and many more. Soft matter is vastly found almost everywhere in our world! Even the biological systems such as membranes, proteins and DNA consist of soft matter. Thus it is very important to study these materials and their properties from not just a physical but biological perspective as well.

From a historical perspective, researchers and scientists in the late 19th and early 20th centuries began studying and exploring the properties of such materials, especially polymers and colloids. However, in the latter half of the 20th century Soft Matter Physics actually gained a lot of traction and emerged as a distinct field of study. One of the pioneering works laying the foundation for the field was the seminal book "The Physics of Polymer Chains" by Paul Flory, published in 1969. This provided a solid theoretical framework for understanding and studying the properties of polymer chains, which are the fundamental units of many soft materials. Around the same time, significant contributions to the study of understanding the dynamics of polymers and their behaviour in entangled systems were also

being made. Especially by researchers like Pierre-Gilles de Gennes, who earned the Nobel Prize in Physics in 1991 for his work on polymers and other soft matter systems, and Samuel Edwards to name a few. In the 1970s and 1980s, the development of advanced experimental techniques, such as light scattering, neutron scattering, and microscopy, allowed researchers to probe the structure and dynamics of soft matter systems at various length and time scales. These experimental advances, coupled with theoretical developments in areas like statistical mechanics and computer simulations, led to a deeper understanding of the complex behavior of soft matter systems.

The study of soft matter physics has been driven by the desire to understand the fundamental principles governing the behavior of these materials, as well as by the numerous applications of soft matter in various fields. For example, polymers are widely used in plastics, rubbers, adhesives, and coatings, while liquid crystals are essential in display technologies. Colloids and emulsions are found in many consumer products, such as paints, cosmetics, and foods. Biological soft matter, such as membranes and proteins, plays a crucial role in understanding the functioning of living systems.

Currently, Soft Matter Physics as a field is at a very exciting stage. It is a very interdisciplinary field bridging multiple disciplines including physics, chemistry, biology, materials science and engineering. It has countless real world applications in many areas of everyday life. With so many technological advancements and more in the future, such a rapidly evolving field has great potential for major contributions in science and research in the future as well!

## 1.2 Polymer Physics

Our work primarily focuses on Polymer Physics which comes under the umbrella of Soft Matter Physics. Polymer physics is a branch of soft matter physics that deals with the study of the structural, dynamic, and physical properties of polymers, which are large molecules composed of repeating units called monomers. Statistical physics lies at the very core of polymer physics, providing a fundamental framework for understanding the behavior and properties of these complex macromolecular systems. The ability to describe the conformational statistics and dynamics of polymer chains, as well as their phase behavior and transitions, hinges upon the powerful tools and principles of statistical mechanics.

One of the central themes in polymer physics is the study of polymer chain conformations and their associated entropy. Polymer chains, with their immense number of monomeric units, possess a staggering number of possible configurations, each contributing to the overall entropy of the system. There are rigorous models, such as the freely jointed chain, worm-like chain, and rotational isomeric state models, to quantify the configurational entropy and predict the dimensions and conformational properties of polymer chains in various environments. The concept of excluded volume, which accounts for the fact that different segments of a polymer chain cannot occupy the same space, plays a crucial role in determining the scaling behavior of polymer chain dimensions. Statistical physics provides analytical and computational approaches to incorporate this non-ideal behavior, enabling accurate predictions of chain sizes and conformations in different solvent conditions.

Furthermore, there are intricate dynamics of polymer chains, which span a vast range of time and length scales. The reptation model, describes the snake-like motions of polymer chains through the constraints imposed by entanglements with neighboring chains. This framework has been instrumental in understanding the viscoelastic behavior and relaxation processes of polymer melts and concentrated solutions. Phase transitions, a fundamental concept in statistical physics, are ubiquitous in polymer systems. The crystallization of polymers, where ordered crystalline regions coexist with disordered amorphous regions, can be understood through the lens of statistical mechanics, which provides insights into the delicate balance between enthalpic and entropic contributions.

Computational approaches, such as molecular dynamics simulations and Monte Carlo methods, have become indispensable tools in polymer physics, complementing theoretical and experimental efforts. These techniques, grounded in statistical mechanics, allow researchers to explore the conformational dynamics, phase behavior, and emergent properties of polymer systems at various length and time scales, bridging the gap between microscopic and macroscopic descriptions.

### 1.3 Why study various Polymer Architectures and their Relaxation properties?

The study of polymer architectures is a vital area within polymer physics, as the molecular architecture of polymers significantly influences their physical properties, conformational behavior, and overall performance in various applications.

The architecture of a polymer chain directly impacts its conformational statistics and entropy. The classic Gaussian chain model, derived from statistical mechanics principles, describes the scaling behavior of linear polymer chains, where the mean-square end-to-end distance scales linearly with the number of monomers. However, as polymer architectures become more complex, such as branched, star-shaped, or cyclic topologies, the conformational behavior deviates from the simple Gaussian chain model, necessitating more sophisticated theoretical treatments. One of the key challenges in studying complex polymer architectures is accounting for the effects of topological constraints and excluded volume interactions.

Studying the relaxation properties of various polymer architectures is of great importance in polymer physics, as it provides crucial insights into the dynamics, rheological behavior, and processing characteristics of these materials. The relaxation processes of polymers span a wide range of time scales, from fast local motions to slow, cooperative chain dynamics, and are intimately tied to their molecular architecture and topological constraints.

My primary motivation for studying relaxation properties of different architectures stems from the research work in Prof. Apratim Chatterji's group. Initially, we were trying to study the segregation properties of a few particular architectures crucial in modeling an E.Coli chromosome as published in Apratim et al.'s work<sup>[4][5]</sup>. Then we felt the need of a better understanding about the dynamics, especially the relaxation dynamics, of those architectures. So we have tried to do an even more fundamental study by starting with absolutely basic polymer architectures like linear-chain and ring polymers and then gradually increase more complexity to study the relaxation properties due to these changes.



## 1.4 Thesis Outline

We have used the basic bead-spring model for our polymers and performed Molecular Dynamics (MD) simulations over it. Our primary focus has been to first study the relaxation properties of a single polymer in open vacuum space instead of a solvent. To exactly mimic such dilute solutions we have to include hydrodynamics of the solvent as well. But we don't address it here in this work since it adds further more complications, while we are trying to study these properties at a very basic level first and then add such complications later once we grasp the basic understanding. We have different architectures which we formed by introducing cross-links within polymers. We study :

- Static property like Radius of Gyration ( $R_g$ ) to get an idea about the size of these polymer architectures.
- Then we study their Diffusion properties and how/if the Diffusion scaling changes across architectures.
- Finally, we address the Conformational relaxation properties of the polymers and compare it across different architectures.



# Chapter 2

## Theory and Methods

### 2.1 Role of Computational Methods

Computational methods play a pivotal role in polymer physics, providing powerful tools to explore the intricate behavior and properties of these complex macromolecular systems. By harnessing the principles of statistical mechanics and leveraging computational power, researchers can gain unprecedented insights into the conformational dynamics, phase behavior, and emergent properties of polymers across various length and time scales.

At the heart of computational approaches in polymer physics lies molecular simulations, which enable the direct modeling and observation of polymeric systems at the molecular level. Molecular dynamics (MD) simulations, based on the laws of classical mechanics and statistical mechanics, have become an invaluable tool for studying the conformational dynamics and structural properties of polymer chains. By integrating the equations of motion for individual atoms or coarse-grained beads, MD simulations provide a detailed picture of how polymer chains move, deform, and interact with their surroundings. Coarse-grained (CG) modeling techniques, which involve representing groups of atoms as single beads or particles, have enabled simulations of larger polymer systems over longer time scales. CG models, parameterized using statistical mechanics principles and informed by atomistic simulations, can capture the essential features of polymer behavior while reducing computational complexity. One of the key strengths of MD simulations in polymer physics is their ability to capture the effects of excluded volume and topological constraints, such as entanglements,

on the conformational statistics and dynamics of polymer chains. These simulations can accurately reproduce phenomena like reptation, which describes the snake-like motions of polymer chains through the constraints imposed by entanglements with neighboring chains. Furthermore, MD simulations provide access to dynamic properties, such as relaxation times and viscoelastic behavior, which are essential for understanding the processing and rheological properties of polymeric materials.

The synergy between computational methods, theoretical models, and experimental techniques has been a driving force in advancing our understanding of polymer physics. Computational approaches provide a powerful means to test and refine theoretical models, while experimental data serves as a benchmark for validating and improving computational methods. This iterative process has led to significant advancements in our ability to predict and design polymeric materials with tailored properties for various applications.

We have performed MD simulations for our bead-spring model of polymers using LAMMPS Molecular Simulation package. We extract the raw data from these simulation runs and then analyze them further to calculate meaningful quantities related to our purpose. Finally, we do statistical averaging of all the data over multiple independent runs and present the final data.

## 2.2 Bead-spring model

The bead-spring model is a very fundamental yet effective model for studying polymer physics. Each monomer is essentially a bead and these monomer beads are connected through harmonic potential springs with a constant spring constant. These harmonic springs mimic the bond between two monomers. This whole system depicts a polymer chain.

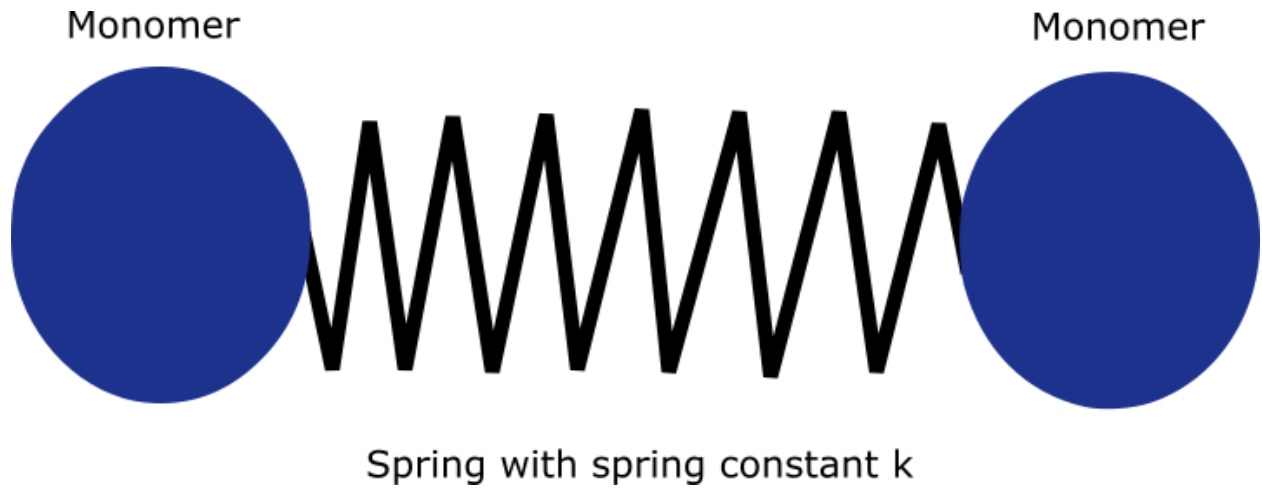


Figure 2.1: Representation of a single bead-spring polymer unit

The spring constant is  $k$  and the equilibrium distance between both the monomers is 1 unit. So for a displacement of  $\delta x$  between the monomers, the potential energy is

$$U = k(\delta x)^2/2$$

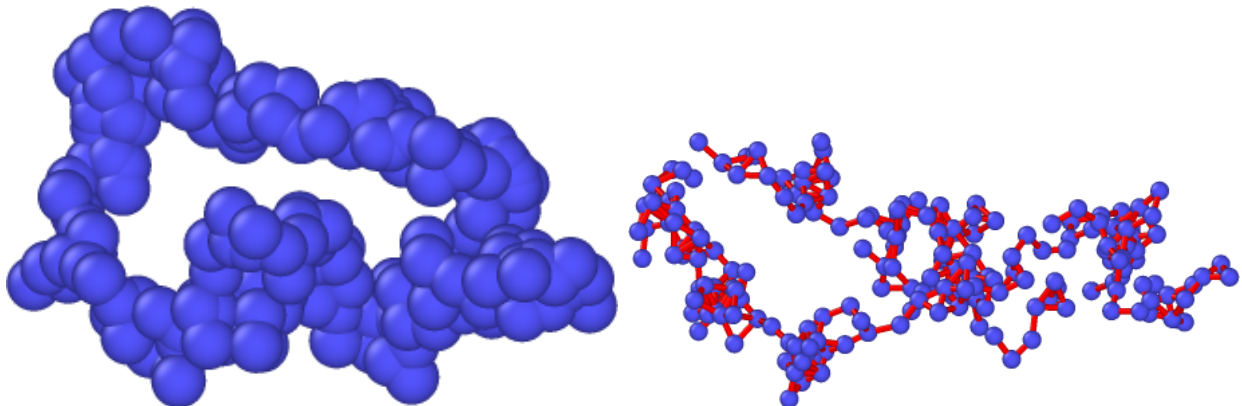


Figure 2.2: Polymer Simulation snapshots

## 2.3 Model Description

### 2.3.1 Molecular Dynamics

Molecular dynamics (MD) simulations have emerged as invaluable tools for exploring the intricate behavior of polymers at the molecular level. Polymers, with their diverse structures and dynamic properties, exhibit complex behaviors that pose significant challenges for experimental investigation. In the realm of computational modeling, the Langevin Dynamics approach plays a pivotal role in elucidating the dynamics and thermodynamics of polymer systems. We look briefly into the intricacies of Langevin Dynamics and its application in MD simulations of polymers.

The essence of Langevin Dynamics lies in its ability to combine deterministic Newtonian mechanics with stochastic fluctuations, effectively modeling the motion of particles in a medium. For polymer systems, Langevin Dynamics captures the intricate interplay between deterministic forces arising from intramolecular interactions and the stochastic effects of thermal fluctuations and solvent interactions. The Langevin equation, a cornerstone of this approach, incorporates these elements to describe the motion of polymer chains in a solvent environment.

The Langevin equation governing the motion of polymer segments can be expressed as<sup>[1]</sup>:

$$m_i \frac{d^2 \mathbf{r}_i}{dt^2} = \mathbf{F}_i - \gamma m_i \frac{d\mathbf{r}_i}{dt} + \eta_i(t) \quad (2.1)$$

Here,  $m_i$  represents the mass of the  $i$ -th polymer segment,  $\mathbf{r}_i$  its position vector,  $\mathbf{F}_i$  the deterministic force acting on it,  $\gamma$  the friction coefficient, and  $\eta_i(t)$  a stochastic force term representing random thermal fluctuations.

The Langevin equation is numerically integrated over small time steps using algorithms like the Verlet integrator. At each time step, deterministic forces, including bonded and non-bonded interactions within polymer chains and with solvent molecules, are computed. Additionally, stochastic forces are introduced to mimic the random collisions experienced by polymer segments. The friction coefficient  $\gamma$  governs the rate of dissipation of kinetic energy due to interactions with the solvent.

We have performed Langevin Dynamics Simulations on various polymer model configurations and architectures (Linear Chain, Ring, Dumbbell etc.). We have used a bead spring polymer model where we have a chain of spherical beads. Each bead has 2 neighbors to which it is connected through harmonic spring interactions :

$$V_{spring} = \kappa(r - a)^2$$

, where  $\kappa = 100k_B T/a^2$  is the spring constant of each spring. 'r' is the distance between two neighbouring monomers. 'a' is the equilibrium length of each spring and is also the unit of length in our simulation. We have used WCA potential to model the excluded volume interactions between the monomers. The diameter/ $\sigma$  for each monomer is equal to 0.8a and the WCA potential is :

$$V_{WCA} = 4\epsilon \left[ \left( \frac{\sigma}{r} \right)^{12} - \left( \frac{\sigma}{r} \right)^6 \right] + \epsilon_0 \quad (\forall r < 2^{1/6} \sigma) \quad (2.2)$$

where  $\epsilon = k_B T$ . The quantity  $\epsilon_0$  ensures that the potential goes to zero smoothly at the cutoff, so that  $V_{WCA} = 0 \forall r$  greater than the cutoff. If the potential cutoff is at  $r = 2^{1/6}$  like we have done here, then  $\epsilon_0 = \epsilon$ .

### 2.3.2 Simulation Model details

We have focused on very dilute solutions (one polymer in open space) with excluded volume interactions. Our LAMMPS script is for an NVE ensemble simulation. We have used Velocity-Verlet Algorithm for numerical integration of equations of motion.

Given the positions  $\mathbf{r}_i$  and velocities  $\mathbf{v}_i$  of particles at time  $t$ , we first predict their positions at a time  $t + \Delta t$  using the current velocities and the Verlet integration formula:

$$\mathbf{r}_i(t + \Delta t) = \mathbf{r}_i(t) + \mathbf{v}_i(t)\Delta t + \frac{1}{2}\mathbf{a}_i(t)(\Delta t)^2 \quad (2.3)$$

where  $\mathbf{a}_i$  is the acceleration of particle  $i$  calculated from the forces acting on it.

With the predicted positions, we compute the forces acting on each particle at time  $t + \Delta t$

using the updated positions. Finally, we use the predicted positions at  $t + \Delta t$  and the forces to update the velocities to  $t + \Delta t$  using the Verlet algorithm:

$$\mathbf{v}_i(t + \Delta t) = \mathbf{v}_i(t) + \frac{1}{2} (\mathbf{a}_i(t) + \mathbf{a}_i(t + \Delta t)) \Delta t$$

where  $\mathbf{a}_i(t + \Delta t)$  is the acceleration of particle  $i$  calculated using the updated forces.

### 2.3.3 LAMMPS Simulation parameters

- Units = LJ units
- $\kappa$  (spring constant) = 100
- $k_B T$  (temperature) = 1
- $a$  (equilibrium bond length) = 1
- $\gamma = 1.0$
- $\epsilon = 1.0$
- $\sigma = 0.8$
- LJ potential cutoff = 0.898 LJ units
- $\eta$  (dilute solvent) = 1.0
- $\Delta t$  (timestep) = 0.01 Simulation time units (STU)
- All of the values related to time calculation in this thesis are reported in terms of  $\tau_0$ , which is equal to 1 simulation time unit. Simulation times are equal to :

No. of LD iterations in the simulation  $\times \Delta t$  (timestep)



## 2.4 Radius of Gyration ( $R_g$ )

The radius of gyration is a fundamental concept in polymer physics that provides a quantitative measure of the size and spatial distribution of a polymer chain. It is a critical parameter for understanding the structural and dynamical properties of polymers. Mathematically, it is expressed as<sup>[7]</sup>:

$$R_g^2 = \frac{1}{2N^2} \sum_{i,j} |\mathbf{r}_i - \mathbf{r}_j|^2 \quad (2.4)$$

where  $N$  is the no. of monomers in the polymer and  $\mathbf{r}_i, \mathbf{r}_j$  are the position vectors of  $i$ th,  $j$ th monomers respectively.

We will use this calculated  $R_g$  to calculate the Diffusion times of the COM of the polymer.

## 2.5 Diffusion related analysis method

Diffusion Constant ( $D$ ) is a measure of how quickly a polymer diffuses<sup>[2]</sup>. We plot the Mean Square Displacement ( $\langle R^2 \rangle$ ) of the polymer vs time for the displacements. We then choose a suitable linear fit range for this plot. Then we find the Slope ( $m$ ) of this linear fit. This gives us the Diffusion Constant,  $D=m/6$ .

The technique used to find the suitable linear fit range is as follows :

- Calculate and plot MSD for the polymer.
- Take derivative of the MSD values and use the slope values to determine linear range for Diffusion Constant calculation by doing semi-log plots and margin for deviation from mean value = 5%.
- Do a linear fit till the calculated/estimated linear range for the MSD plot and calculate Diffusion constant and Diffusion Relaxation time.

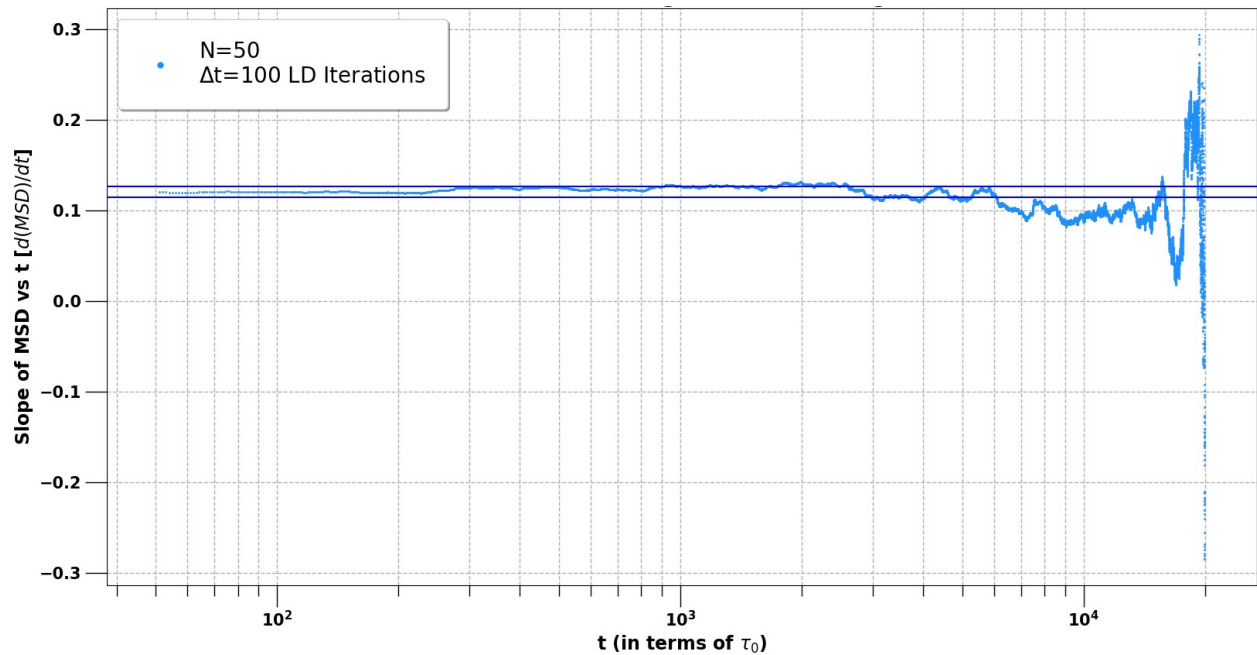


Figure 2.3: An example plot to demonstrate linear range calculation through derivative (with respect to time) of MSD plot :  $d(MSD)/dt$  vs  $t$  for Linear Chain (with log-x axis and averaged over 25 runs)

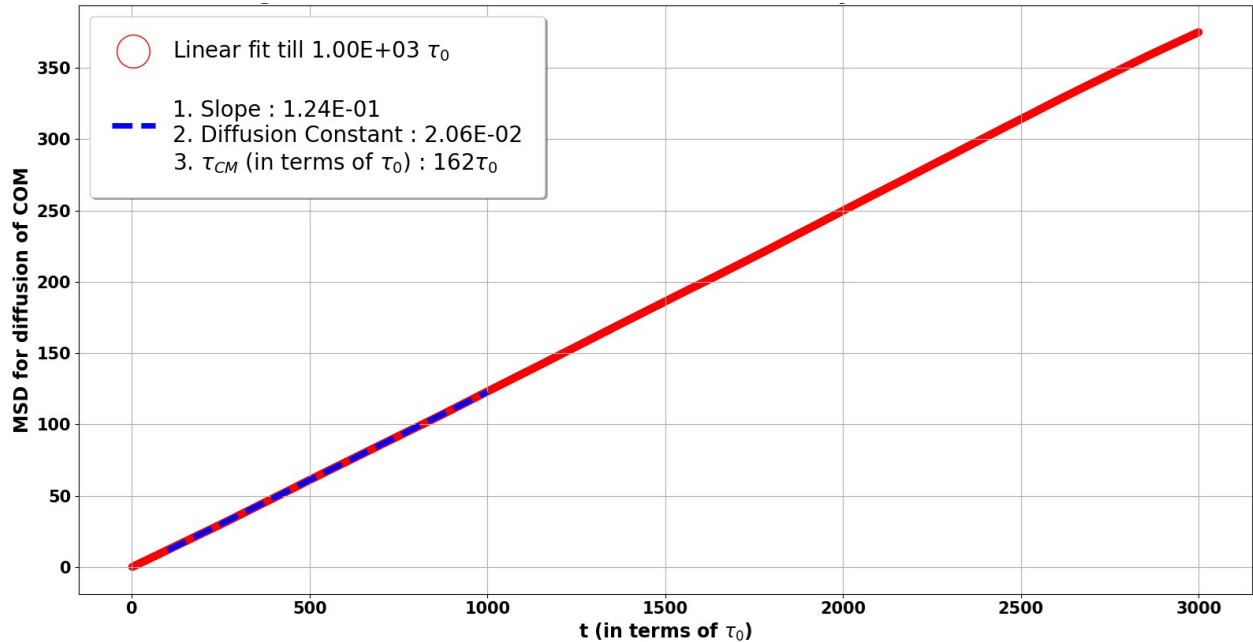


Figure 2.4: An example plot to demonstrate MSD plot for diffusion (LD data with linear fit only in diffusive regime and initial ballistic regime is not included) : Avg MSD vs  $t$  for Linear Chain ( $N=50$  and data taken every 100 LD iterations)

After getting a rough estimate for our linear fit range, we use it to fit it on the original MSD plot and extract the slope.

The diffusion time is a characteristic time scale that describes the time required for a polymer chain to explore its configurational space through diffusive motion. The diffusion time for a polymer chain is typically defined as the time required for the center of mass of the polymer to diffuse a distance equal to its own radius of gyration ( $R_g$ ). Mathematically, the diffusion time ( $\tau_{diff}$ ) can be expressed as<sup>[8]</sup>:

$$\langle R_g^2 \rangle = 6D\tau_{diff} \quad (2.5)$$

## 2.6 Vector conformation relaxation analysis method

Conformation Relaxation time ( $\tau_{conf}$ ) refers to the time taken by a polymer to attain equilibrium in terms of its conformational configuration. This means that the polymer becomes indistinguishable from its initial conformation over the perturbations. There is an exponential decay relation between the autocorrelation function and time<sup>[3]</sup> :

$$\langle \mathbf{R}(t) \cdot \mathbf{R}(t + dt) \rangle = \exp(-t/\tau) \quad (2.6)$$

This decay function looks like this after plotting :

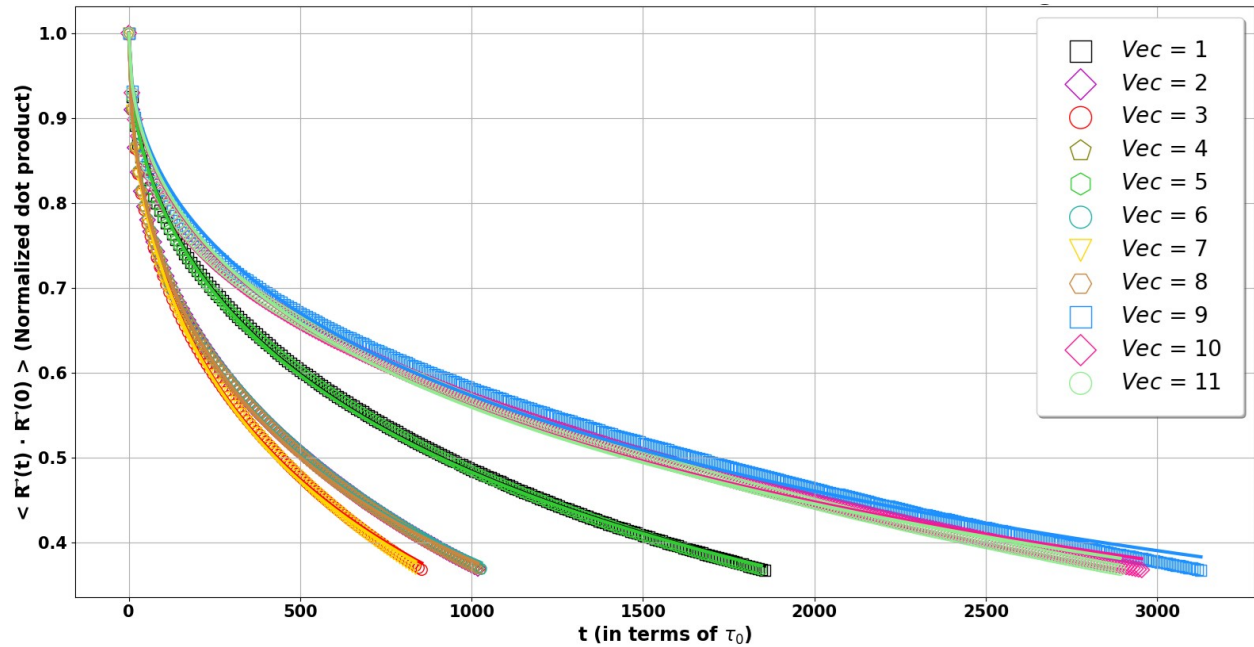


Figure 2.5: An example of Normalized autocorrelation plot for different vectors of "Inverted-8" (I8)/Dumbbell Architecture : Normalized autocorrelation function vs  $t$  for vector relaxation of Dumbbell ( $N=100$  and averaged over 25 runs)

- For Conformation Relaxation Times we plot normalized time autocorrelation vs  $t$ . So we plot  $\langle \mathbf{R}(t) \cdot \mathbf{R}(t + dt) \rangle$  vs  $t$  (in terms of  $\tau_0$ ) where  $\mathbf{R}$  is a vector spanning the polymer for its conformation.
- Then we do its semi-log plot with natural log of y-axis to convert the exponential decay to linear scale.
- Finally, we roughly get an idea of a linear range and fit a linear regression till that range to extract the slope of this linear range.
- This slope is equal to  $-1/\tau$  where  $\tau$  is the desired relaxation time

The semi-log plot looks like this after linear fit :

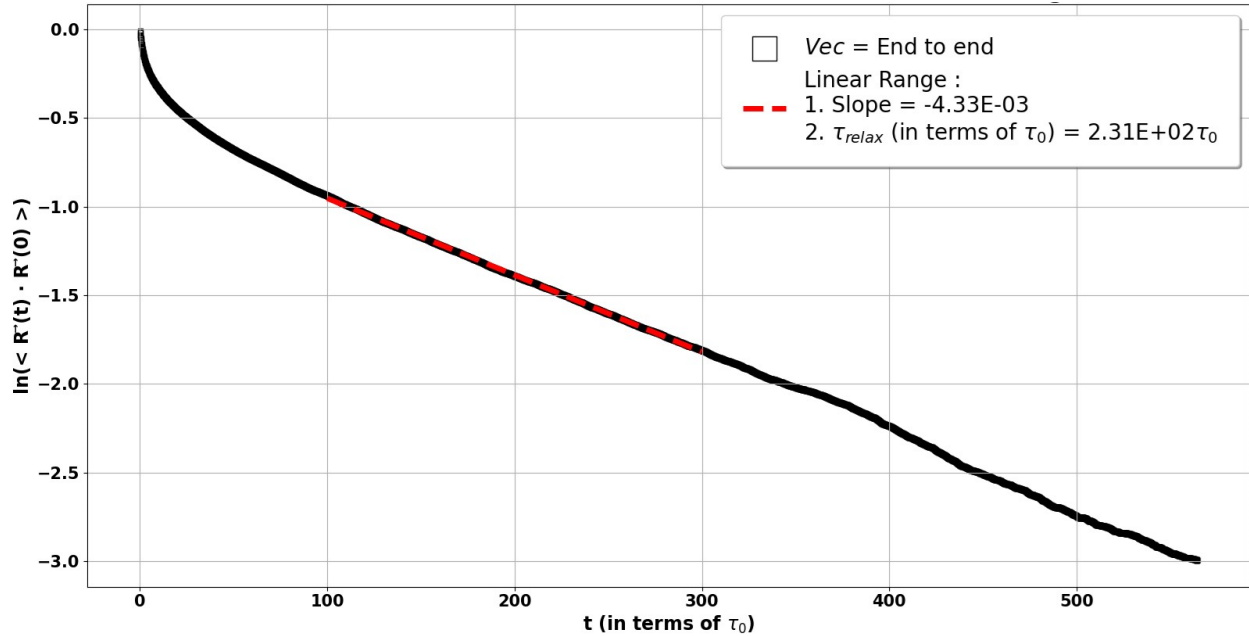


Figure 2.6: An example of semi-log plot of Normalized autocorrelation vs  $t$  for Linear Chain ( $N=50$  and averaged over 25 runs)

## 2.7 Various Architectures Used

For Diffusion related study it is relatively simple to just keep track of the COM and calculate the desired quantities. But things get tricky with vector conformation relaxation related calculations. With increasingly more complex architectures the amount of vectors to analyze also increases. Thus one needs to keep track of all these vectors separately and calculate their relaxation times to get more insights about the conformations of the polymer and obtain any possible trends. We mention all the four architectures used in our study with information about all the useful vectors :

### 2.7.1 Linear Chain

The Linear Chain is just a series of bead spring units connecting in a linear fashion to make a chain like structure. Its two ends are disjoint and the monomers motion is restricted subject to the springs it is attached. During the simulation or while studying its dynamics, we can

see that the linear chain is flexible and free to take countless arbitrary configurations making a worm-like structure. Linear Chain is quite extensively used to do polymer physics related studies. It is arguably the simplest Polymer architecture and has a plethora of research done and still being done about its properties. It also serves as a nice fundamental architecture for our study across the other architectures. It can be the fundamental polymer architecture to which we add further complications and modified topology by adding more cross-links and further complications.

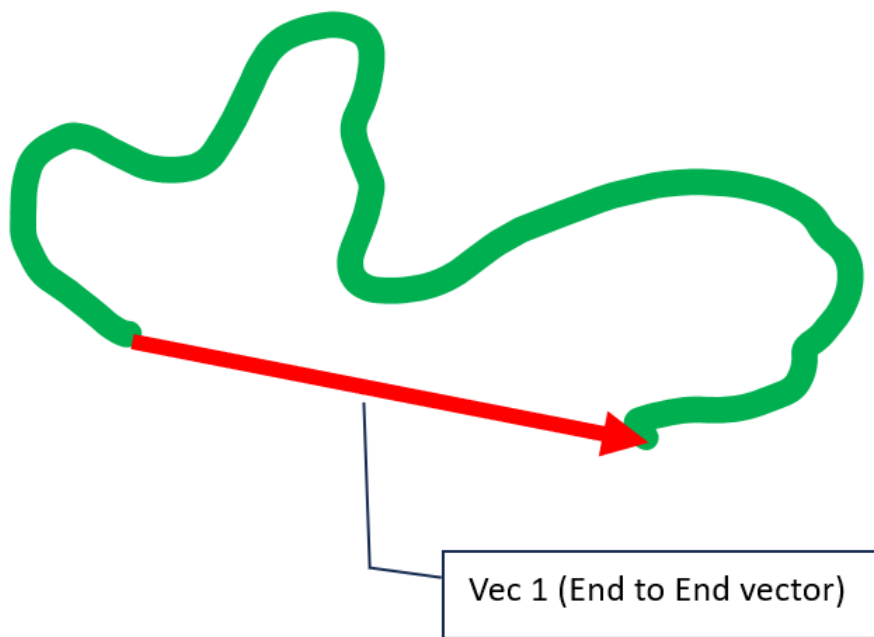


Figure 2.7: Vector used for  $\tau_{Conf}$  calculation

For Diffusion the idea is relatively straight forward. We just keep track of the motion of the Centre of Mass of this Linear Chain polymer with its unwrapped coordinates and perform the diffusion related analysis as we have described already in above sections. But for Conformation Relaxation related study we discussed above that we need vectors across the polymer to study its conformation. So for Linear Chain we have used the End-to-end vector to study. This vector just spans the whole contour length of the polymer chain spanning from the first monomer of the chain to the last monomer as we can see in [Figure

2.7].

### 2.7.2 Arc0/Ring Polymer

The Arc0/Ring Polymer is just a Ring like structure of polymer architecture where we connect the two ends of a Linear Chain to make it like a ring or a closed/jointed loop thus leaving no loose ends. We do this by introducing one more spring to the Linear Chain by joining the two end monomers together. Just like a Linear Chain this is also flexible and free to take countless arbitrary configurations but always keeping the loop intact. Ring polymer is also studied quite a lot in Polymer physics. It is relatively quite simpler but very effective to study polymer dynamics and very applicable as well in a lot of other studies. It is definitely of the most fundamental architectures to study along with Linear Chain.

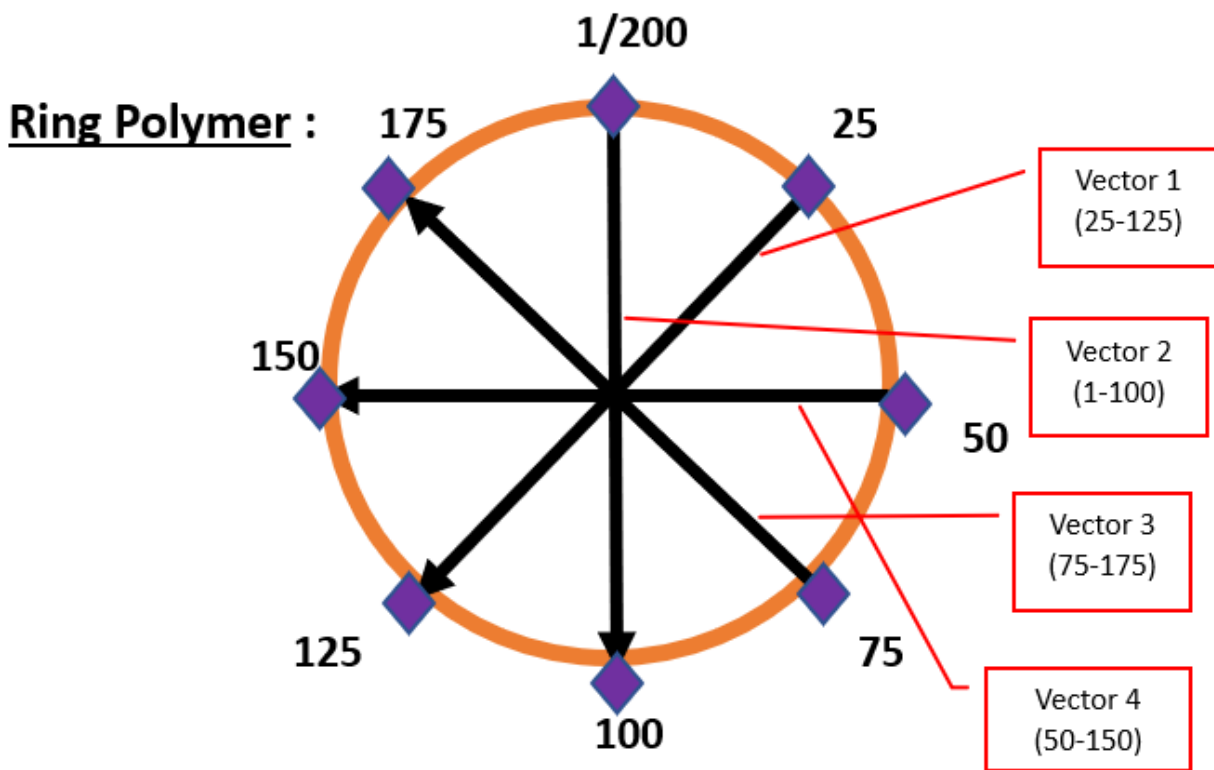


Figure 2.8: Ring Schematic

Diffusion study for Ring polymer is also very similar to Linear Chain or in fact any other architectures by keeping track of the Centre of Mass of the Polymer and proceeding with

techniques explained in previous sections. But here, the Conformation Relaxation related study is a bit different than Linear Chain. There we were able to use the End-to-End vector but for a Ring there is no such End-to-End vector. The End-to-End vector will just depict a normal bond between any two monomers of the Ring, since it is Homopolymer and a cyclic polymer. This is why we choose to study the "Diametric" vectors of this Ring. By "Diametric" we mean a vector connecting any two of the farthest monomers according to the contour length of the polymer as shown in [Figure 2.8]. This is the longest possible vector (based on contour length) Later on throughout the simulation the Ring is going to take a lot of different configurations and our vector might keep on changing length and directions as well. But the vector is always between those two chosen monomers only.

Now that we have decided what kind of vector we want, we can choose countless such "Diametric" vectors Each of them should giving statistically very similar results. So just for better averaging, we choose four such different vectors as shown in [Figure 2.8] and then take the average of all of their individual results. Both of our next two architectures are essentially derived from the Ring Polymer itself by just introducing cross-links in the Ring Polymer. Also, this same concept of "diameter" like vectors will be used there as well.

### 2.7.3 "Inverted-8"(I8)/Dumbbell Polymer

The "Inverted-8"/Dumbbell polymer architecture consists of just 1 more extra cross link than Ring Polymer. We join any one pair of monomers of the "Diametric" vector of the Ring polymer. This essentially makes a figure something like two small ring-like loops connected at one common junction point of monomers looking like an "inverted-eight/ $\infty$ " configuration as shown in [Figure 2.9].

This configuration is basically two equally sized loops (in terms of contour length) but each having half the contour length of the whole polymer joint together. So we can have 4 different vectors just like a Ring polymer for each of the individual small loops and study the relaxation properties of these vectors separately to see how the conformation dynamics change within these small loops as well. These small loop vectors are basically spanning the whole small loop like a "diameter". So we have 8 such vectors (as shown in [Figure 2.9]) and we expect one group of 4 vectors for a particular small loop should give similar results to group of the other 4 vectors for the other small loop over a statistically averaged data.



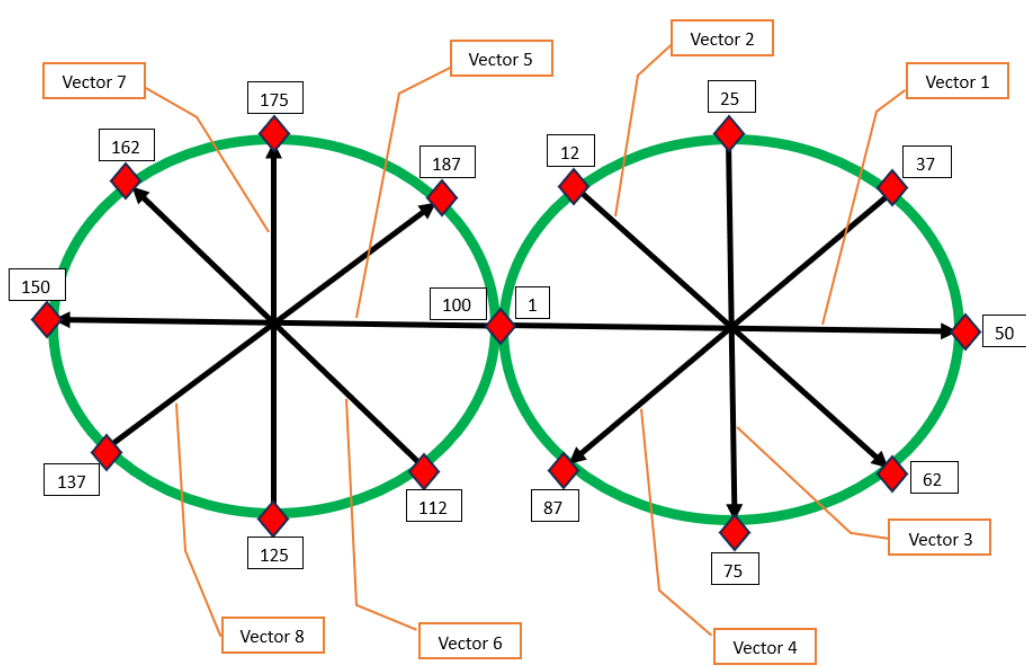


Figure 2.9: "Inverted-8" (I8)/Dumbbell loop vectors

Also, other than the small loops, we need some vectors which can somewhat span the whole "Inverted-8"/Dumbbell polymer as well. Similar to our concept of "Diameter" like vectors, we try to have a vector with the longest contour length for the whole polymer. Now keep in mind that we have a cross-link in between the polymer. So we have to keep that in account accordingly while comparing the contour lengths of vectors with respect to number of monomers. For example, according to [Figure 2.10] if we choose a vector between monomer 1 and monomer 100 then for a ring that is definitely the longest vector (contour length wise) but here in this case it is literally just a bond vector thus being the smallest vector. This is why we choose the "diameter" like vectors as shown in [Figure 2.10]. Here clearly the Vectors 10 and 11 are smaller than the vector 9 (which is the longest contour length wise) but these vectors can provide more details about the conformation dynamics of the whole polymer as well.

We see that introducing just one single cross link to our fundamental Ring polymer architecture provides us with such a variety of vectors to study and we can extract interesting details through them. It always becomes more and more tricky and complicated when we introduce more and more complications to our architectures by these modified topologies as we will see in the next case of Arc2 polymer architecture.

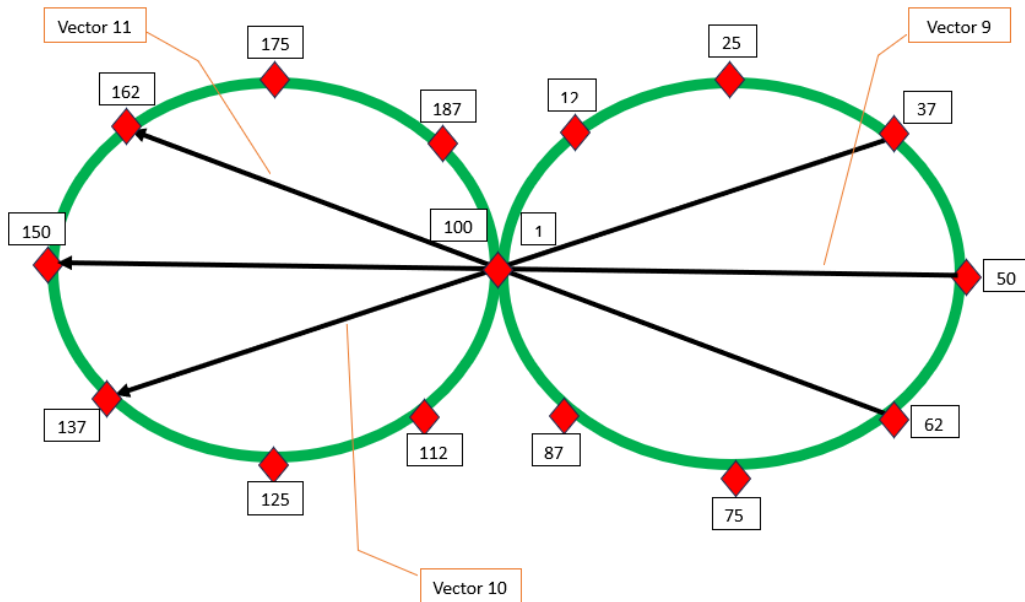


Figure 2.10: "Inverted-8" (I8)/Dumbbell diametric vectors

We have provided the details of all the vectors that we have chosen along with which monomers are involved for those vectors. We have taken an example of a "Inverted-8"/Dumbbell polymer of total 200 monomers and mentioned all the vectors for this particular example accordingly in the [Table 2.1].

- $LoopA : [Monomer1] \rightarrow [Monomer100]$
- $LoopB : [Monomer101] \rightarrow [Monomer200]$
- Vectors 1-8 are vectors within the smaller loops and of contour length 50 monomers each
- Vectors 9-11 are vectors spanning the whole polymer across both the loops, much like a diametric vector for a ring polymer, and of contour length 100 monomers each

Vector	Monomers	Vector	Monomers
1	(1 → 50)	7	(125 → 175)
2	(12 → 62)	8	(137 → 187)
3	(25 → 75)	9	(50 → 150)
4	(37 → 87)	10	(37 → 137)
5	(100 → 150)	11	(62 → 162)
6	(112 → 162)		

Table 2.1: Vectors detail for "Inverted-8"/Dumbbell polymer architecture

## 2.7.4 Arc2 Polymer

The Arc2<sup>[4]</sup> polymer architecture is important for us to study since that is where our motivation to study the dynamics of these different architectures came in the first place. Arc2 was the primary architecture used to study the E.Coli Chromosome in Apratim et al.'s work, later on modified as Arc2-2 for better understanding. So if we study the dynamics of the Arc2 polymer architecture then we can use this knowledge and these results to study the chromosome segregation study more effectively.

The Arc2 polymer architecture consists of 2 more extra cross links than Ring Polymer. But here all the loops and the cross-links are not actually symmetric. The two small loops are equal in size and symmetric to each other but the large loop is twice the size of each of these small loops. So we have total 3 loops and all of these loops connect with each other at the same junction as shown in [Figure 2.11]. This looks like a "bunny-face" type of structure. We have chosen total 15 vectors here. 4 vectors for one small loop, 4 vectors for the other small loop and 4 vectors for the larger loop. The other 3 vectors span across the different loops while trying to maximize the contour length as well. The concept is similar as the "diameter" vector concept but there is no such "diameter" like vector here really which

spans the whole polymer as well. This is why it becomes tricky which vectors to choose to study.

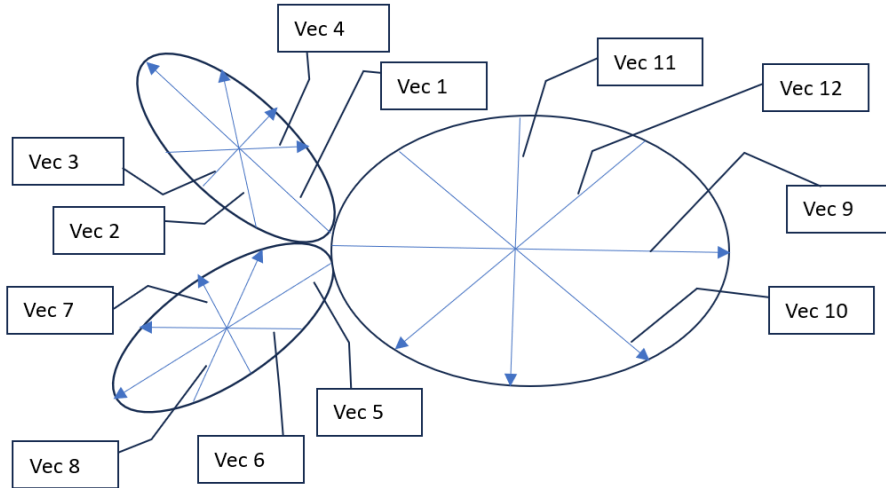


Figure 2.11: Arc2 loop vectors representation

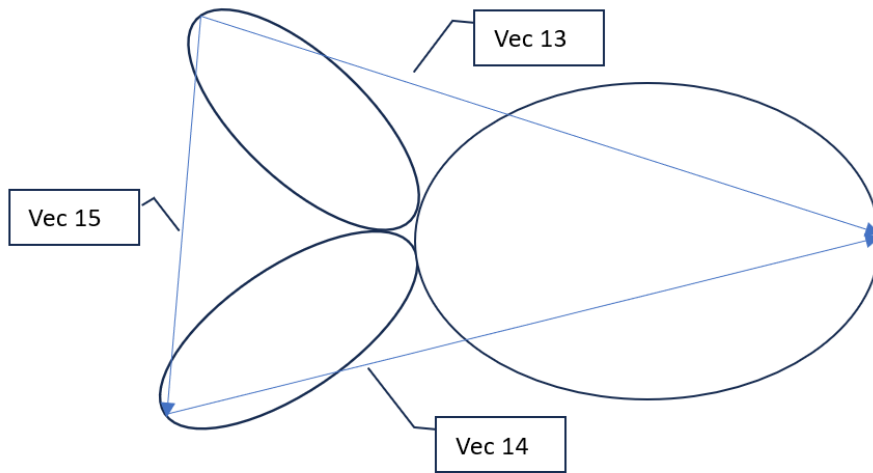


Figure 2.12: Arc2 diametric vectors representation

Vectors 1-8 have the similar concept as the small loop vectors in "Inverted-8"/Dumbbell polymer architecture. Even the larger loop vectors 9-12 follow the same concept with only

difference of them being twice the size (in terms of contour length) of a small loop vector. While vectors 13-15 consists of the vectors connecting the different pairs of monomers of different loops with each other. Thus we have used all 3 such possible vectors to study.

- **Loop C is the larger loop.**
- **Loop A and B are the smaller loops**
- **Vector : 1,2,3,4 for Loop A**
- **Vector : 5,6,7,8 for Loop B**
- **Vector : 9,10,11,12 for Loop C**

We see that 2 more cross links to our fundamental Ring polymer architecture increases the complexity even further with many more vectors to study and analyze. We can always increase such complications even further and try to study the more complicated cases according to our needs of particular architectures. But we will have to be careful about how we proceed with our approach and then extract meaningful results out of it. That is the most challenging part.

- *LoopA* : [Monomer1]  $\rightarrow$  [Monomer125]
- *LoopB* : [Monomer375]  $\rightarrow$  [Monomer500]
- *LoopC* : [Monomer125]  $\rightarrow$  [Monomer375]
- Vectors 1-8 are vectors within the smaller loops
- Vectors 9-12 are vectors within the larger loop
- Vectors 13-15 are vectors spanning the whole polymer across the loops, much like a diametric vector for a ring polymer

We have provided the details of all the vectors that we have chosen along with which monomers are involved for those vectors. We have taken an example of a "Inverted-8"/Dumbbell polymer of total 200 monomers and mentioned all the vectors for this particular example accordingly in the [Table 2.2].

Vector	Monomers	Vector	Monomers
1	(1 → 63)	9	(126 → 251)
2	(17 → 79)	10	(157 → 282)
3	(32 → 94)	11	(189 → 314)
4	(48 → 110)	12	(220 → 345)
5	(376 → 438)	13	(63 → 251)
6	(392 → 454)	14	(251 → 438)
7	(407 → 469)	15	(63 → 438)
8	(423 → 485)		

Table 2.2: Vectors detail

# Chapter 3

## Radius of Gyration

As we already discussed above in previous chapter, study of Radius of Gyration is always quite important whenever we are trying to study the polymer architectures. We should always first have an idea and data about the size of our polymer architecture before we proceed further and Radius of Gyration is always a useful data to have regarding the size of a polymer. One obvious thing we can say point is that as we increase the number of monomers in our polymer, the size of the polymer increases. Thus the increase in Radius of Gyration ( $R_g$ ) is also proportional to the increase in the number of monomers ( $N$ ). But the main question here always is what is the scaling factor or the scaling law for this relation? If we have a relation between Radius of Gyration and Number of monomers like this :  $R_g \propto N^\nu$ , then what is the value of  $\nu$  here? And we don't just have to address it for just one type of polymer architecture. We want to find out how/if the scaling changes for the different polymer architectures as well.

Now according to theory, the Flory exponent  $\nu \approx 0.59$  for a self-avoiding random walk in 3-D space. This is for a polymer chain in dilute systems. So we try to check and verify this scaling for our case as well. We then try to compare the scaling and sizes of polymers across the different architectures also. By this data, we should get an idea of the size of our polymer architectures too which we will use for our Diffusion scaling study in the next chapter.

### 3.1 Comparing $R_g$ data across various architectures

The  $R_g$  data in [Table 3.1] clearly suggests that the polymer architectures affect the sizes of the polymers. We can see that Linear Chain has the highest values of  $R_g$  generally and it gradually keeps on decreasing as we keep making our polymer architecture more and more compact by introducing more cross-links. We can have following general conclusion while comparing the sizes/ $R_g$  values of different polymer architectures :

$$\text{Linear Chain} > \text{Ring} > \text{Dumbbell} > \text{Arc2}$$

Also, the obvious trend of increase in size with increase in number of monomers across a particular polymer architecture is also clearly apparent.

N	Linear Chain		Ring		Dumbbell		Arc2	
	$R_g$	$\sigma_{Rg}$	$R_g$	$\sigma_{Rg}$	$R_g$	$\sigma_{Rg}$	$R_g$	$\sigma_{Rg}$
50	4.47	0.09	3.32	0.01	3.07	0.01	2.79	0.01
100	6.89	0.26	4.59	0.007	4.66	0.06	4.19	0.03
200	10.33	0.39	7.72	0.07	7.05	0.06	6.35	0.04
300	13.51	0.84	9.92	0.16	9.03	0.13	8.07	0.09
500	17.80	1.52	13.34	0.39	12.31	0.30	10.92	0.15
1000	27.97	3.33	20.28	0.69	18.47	0.68	16.70	0.46
2000	41.56	5.93	30.81	2.99	28.17	1.99	25.08	1.32

Table 3.1: Radius of Gyration ( $R_g$ ) data

We also do a log-log plot of this Radius of Gyration vs Number of Monomers data to check the scaling of the Flory exponent  $\nu$ .



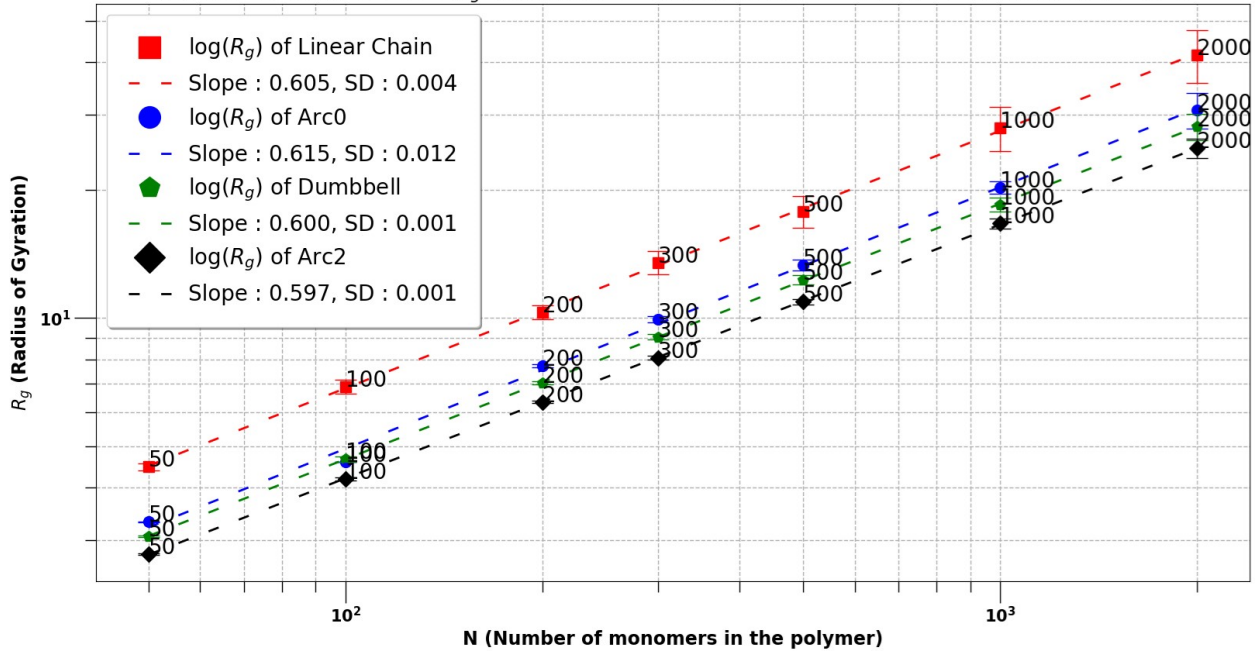


Figure 3.1: log-log Comparison of  $\log(R_g)$  for Polymer Configurations vs  $\log(N)$

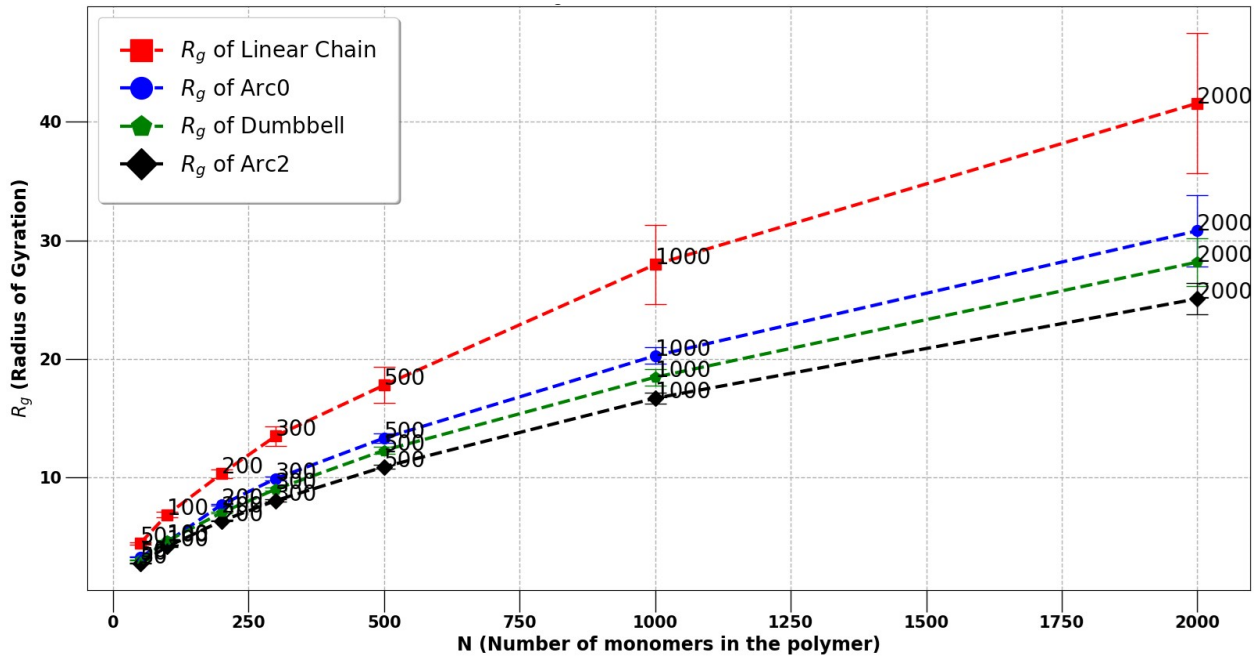


Figure 3.2: Comparison of  $R_g$  for Polymer Configurations vs  $N$

Having a log-log plot [Figure 3.1] converts the Radius of Gyration vs Number of monomers plot to linear scales. We do a scatter plot of all the data points we have and then do linear

regressions over these scatter plots for their respective polymer architectures. We have mentioned their respective slopes as well in the legend of the plots. These values of slopes are the Flory exponents for their respective polymer architectures.

We can see that the Flory exponents for all of our architectures  $\nu \approx 0.6$ , quite similar to the predictions of theory. One more interesting thing to note is that the scaling law and Flory exponent doesn't change even when the polymer architecture is different. So throughout the different architectures, the Radius of Gyration vs Number of Monomers scaling is relatively unaffected. So finally the scaling law becomes :

$$Rg^2 \approx N^{6/5}$$

We can see this scaling relation in the comparison plot of Radius of Gyration (Rg) vs Number of Monomers (N) in [Figure 3.2].

# Chapter 4

## Diffusion Scaling

Now we focus on the diffusion of Centre of Mass of the whole polymer. We will discuss about the Diffusion Constant ( $D$ ) values of the polymer architectures and compare these values across the different architectures we have. Diffusion Constants basically tells us about how fast a polymer diffuses. So it will be interesting to see how the speed of diffusion of a polymer is affected once we change it's architecture.

Then we will also discuss about the Rouse relaxation times for diffusion of these polymers and again compare these time values as well across the different architectures. This is basically the time taken by a polymer to diffuse a distance of  $R_g$  units where  $R_g$  is the Radius of Gyration of that particular polymer architecture.

### 4.1 Comparison of Diffusion Constants ( $D$ )

The Diffusion constants ( $D$ ) data gives a very interesting result. We can see that for a particular value of number of monomers ( $N$ ), the diffusion constant across architectures is almost identical as we can see the data in [Table 4.1]. This means that despite having different polymer architectures with modified topologies and different number of cross-links their diffusion speed is almost identical! So the diffusion speed solely depends on the number of monomers.

N	$D(\text{LinearChain})$	$D(\text{Arc0})$	$D(\text{Dumbbell})$	$D(\text{Arc2})$
50	$2.06 \cdot 10^{-2}$	$2.07 \cdot 10^{-2}$	$2.01 \cdot 10^{-2}$	$2.05 \cdot 10^{-2}$
100	$9.74 \cdot 10^{-3}$	$9.64 \cdot 10^{-3}$	$9.68 \cdot 10^{-3}$	$1.04 \cdot 10^{-2}$
200	$5.33 \cdot 10^{-3}$	$4.95 \cdot 10^{-3}$	$5.05 \cdot 10^{-3}$	$5.16 \cdot 10^{-3}$
300	$3.30 \cdot 10^{-3}$	$3.19 \cdot 10^{-3}$	$3.40 \cdot 10^{-3}$	$3.46 \cdot 10^{-3}$
500	$2.03 \cdot 10^{-3}$	$2.01 \cdot 10^{-3}$	$2.08 \cdot 10^{-3}$	$2.06 \cdot 10^{-3}$
1000	$9.93 \cdot 10^{-4}$	$9.84 \cdot 10^{-4}$	$1.02 \cdot 10^{-3}$	$1.01 \cdot 10^{-3}$
2000	$5.05 \cdot 10^{-4}$	$5.10 \cdot 10^{-4}$	$5.04 \cdot 10^{-4}$	$5.18 \cdot 10^{-4}$

Table 4.1: Diffusion Constant (D) data

Also, we do the same log-log plot analysis [Figure 4.1] again as we did for the Radius of Gyration to check the scaling of Diffusion Constants (D) with respect to the number of monomers (N). The log-log plot comparison converts the data to linear scales for easier extraction of the scaling exponents. We then similarly do the linear regression on the scatter plot and the slopes of these linear regressions give us the scaling exponent for the diffusion constant (D) vs Number of monomers (N) for their respective polymer architectures.

We see that for all of the architectures, the slopes are almost exactly equal to -1. This is also quite accurate as predicted according to the theory since D is always inversely proportional to N according to theory. Also similar to Radius of Gyration data, the scaling law doesn't change even when the polymer architecture is different. So throughout the different architectures, the Diffusion Constant vs Number of Monomers scaling is relatively unaffected (In fact Marcus Muller in one of his works also showed this for Ring and Linear polymers in isolated systems with no hydrodynamics<sup>[6]</sup>. So finally the scaling law becomes :

$$D \approx 1/N$$

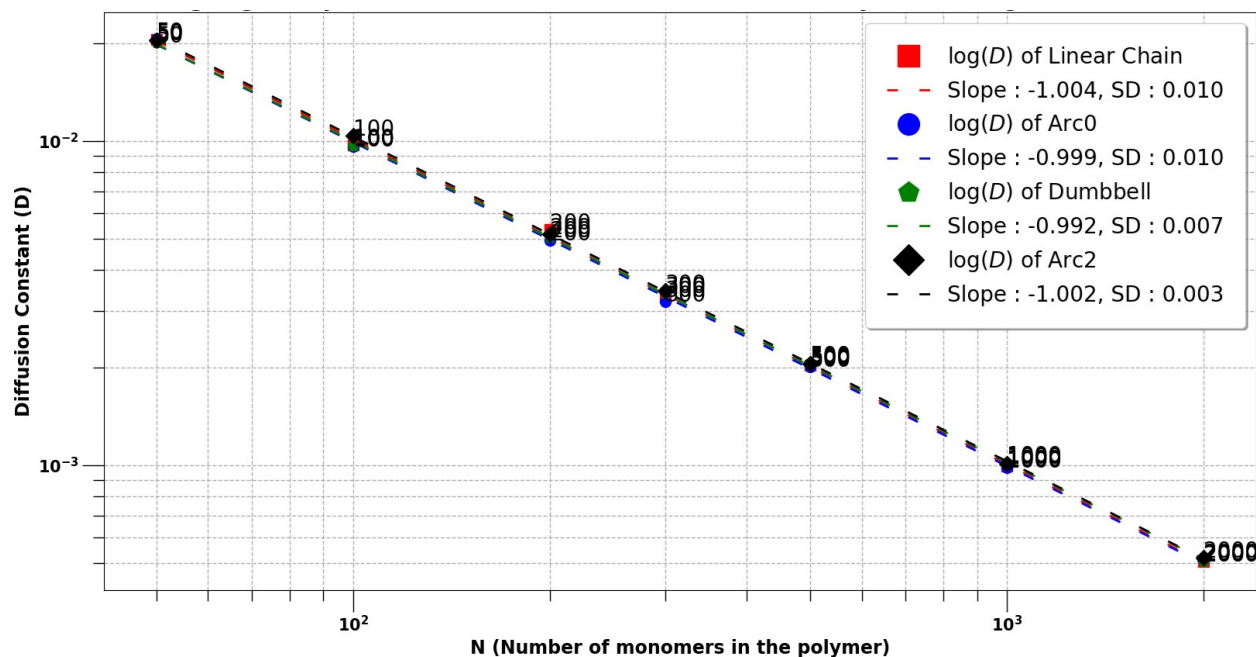


Figure 4.1: log-log Comparison of Diffusion Constant  $\log(D)$  for Polymer Configurations vs  $N$

We can clearly see this scaling relation in the comparison plot of Diffusion Constant (D) vs Number of Monomers (N) in [Figure 4.2].

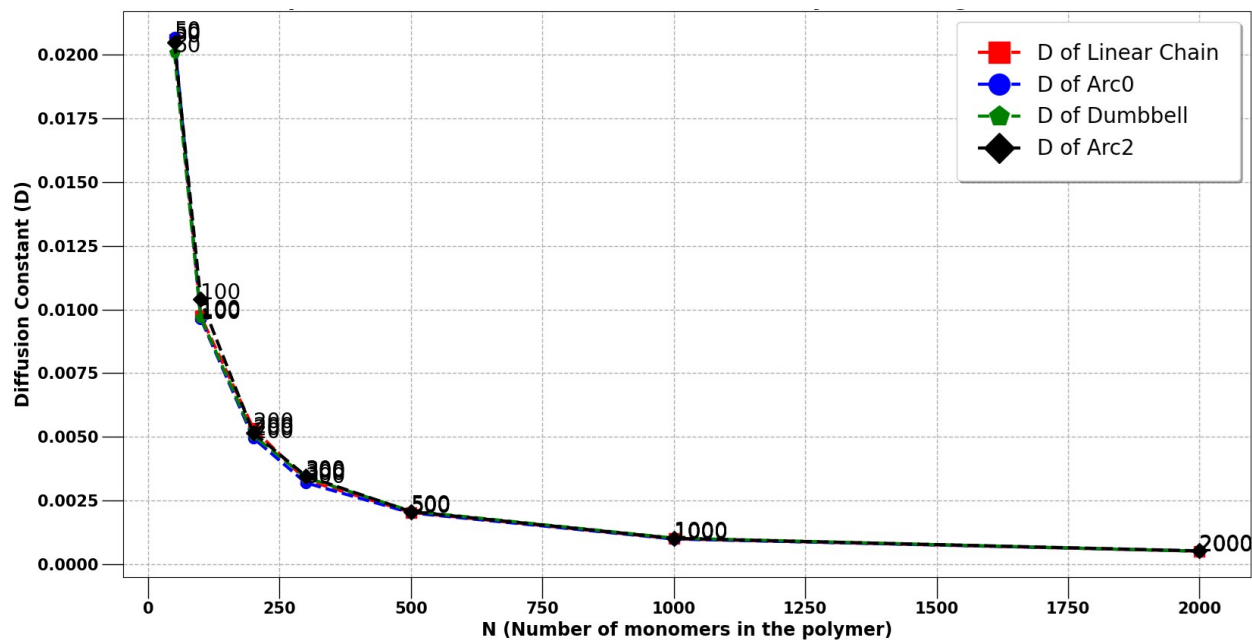
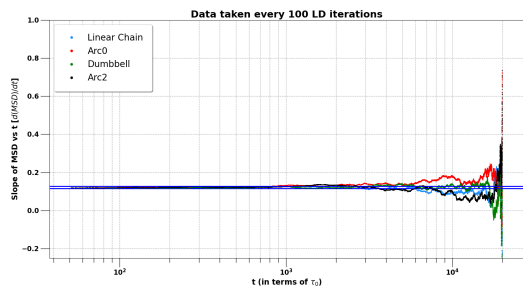
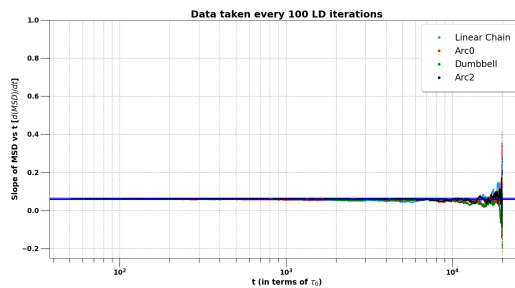


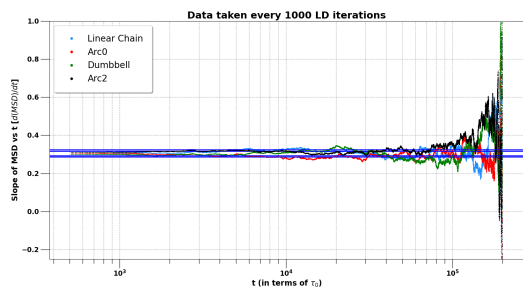
Figure 4.2: Comparison of Diffusion Constant (D) for Polymer Configurations vs  $N$



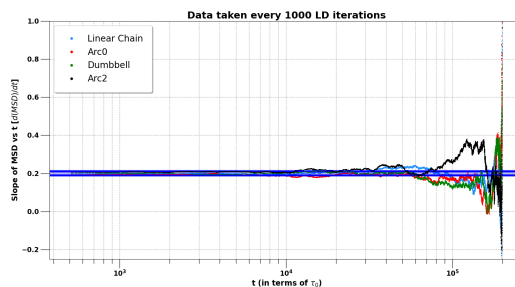
(a)  $N=50$



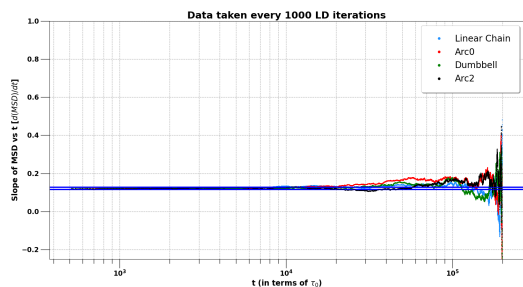
(b)  $N=100$



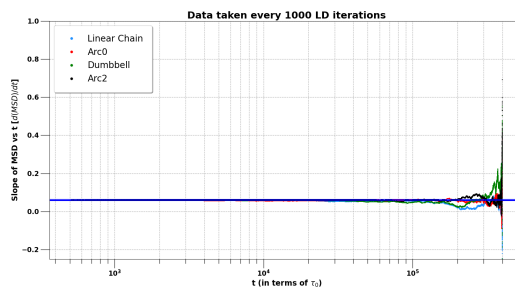
(c)  $N=200$



(d)  $N=300$



(e)  $N=500$



(f)  $N=1000$

Figure 4.3: Plots for  $\text{MSD}/t$  vs  $t$  comparison across various architectures for different cases of No. of monomers in the polymer

## 4.2 Comparison of Diffusion times ( $\tau_{diff}$ )

Now if we look at the diffusion times, based on the data and results we saw above, we should already have gotten an idea of what is going to happen here. For Diffusion times,

$$\langle R_g^2 \rangle = 6D\tau_{diff}$$

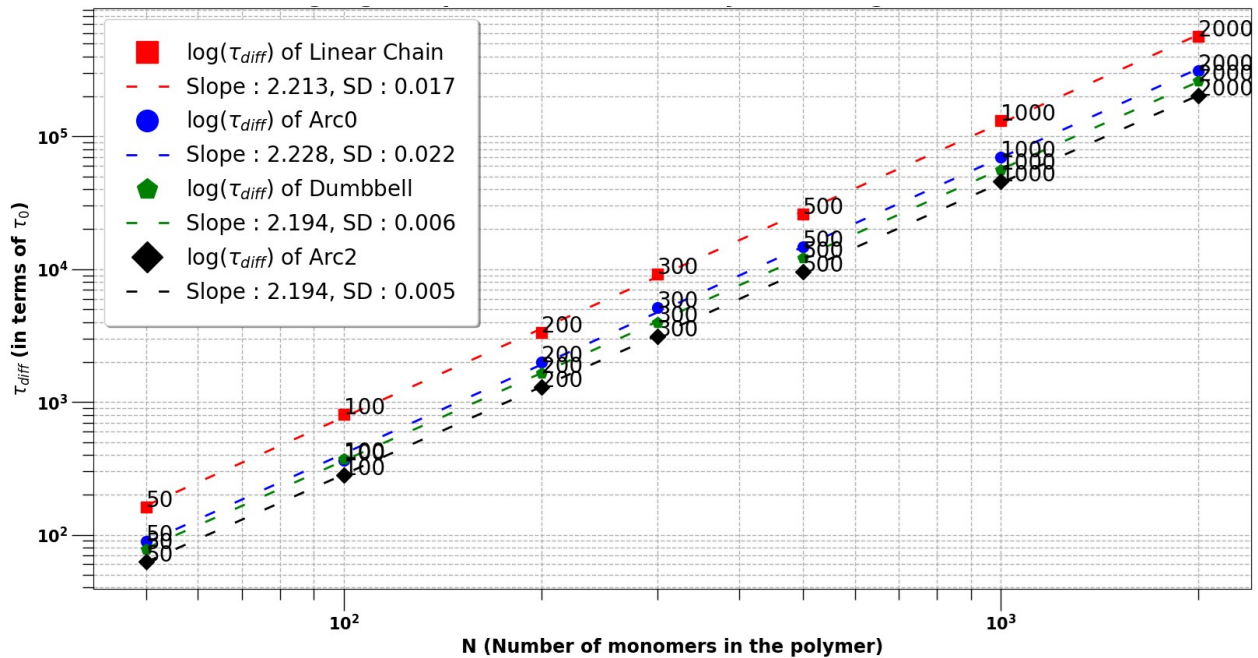


Figure 4.4: log-log Comparison of  $\log(\tau_{Diffusion})$  for Polymer Configurations vs  $\log(N)$

We have already calculated the  $R_g$  values. So we'll use those values to calculate  $\tau_{diff}^{Polymer}$  for each polymer architecture. But the interesting result we found in last section was that the Diffusion Constant ( $D$ ) across the architectures is almost identical. That means if we compare diffusion times across the polymer architectures, the diffusion constant basically plays no role in it. But the  $R_g$  values obviously differ a lot since the sizes of the polymer architectures are actually different. So according to the formula from theory, we can say that the most dominant factor for the differing values of diffusion times across architectures is mainly because of Radius of Gyration values only.

N	$\tau_{diff}(LinearChain)$	$\tau_{diff}(Arc0)$	$\tau_{diff}(Dumbbell)$	$\tau_{diff}(Arc2)$
50	162 $\approx 1.62 \cdot 10^2$	89 $\approx 0.89 \cdot 10^2$	78 $\approx 0.78 \cdot 10^2$	63 $\approx 0.63 \cdot 10^2$
100	812 $\approx 8.12 \cdot 10^2$	364 $\approx 3.64 \cdot 10^2$	374 $\approx 3.74 \cdot 10^2$	282 $\approx 2.82 \cdot 10^2$
200	3337 $\approx 3.33 \cdot 10^3$	2005 $\approx 2.00 \cdot 10^3$	1642 $\approx 1.64 \cdot 10^3$	1303 $\approx 1.30 \cdot 10^3$
300	9223 $\approx 9.22 \cdot 10^3$	5134 $\approx 5.13 \cdot 10^3$	4003 $\approx 4.00 \cdot 10^3$	3134 $\approx 3.13 \cdot 10^3$
500	26060 $\approx 2.60 \cdot 10^4$	14730 $\approx 1.47 \cdot 10^4$	12151 $\approx 1.21 \cdot 10^4$	9632 $\approx 0.96 \cdot 10^4$
1000	131296 $\approx 13.12 \cdot 10^4$	69667 $\approx 6.96 \cdot 10^4$	55895 $\approx 5.58 \cdot 10^4$	45818 $\approx 4.58 \cdot 10^4$
2000	569535 $\approx 5.69 \cdot 10^5$	310334 $\approx 3.10 \cdot 10^5$	262624 $\approx 2.62 \cdot 10^5$	202205 $\approx 2.02 \cdot 10^5$

Table 4.2: Rouse relaxation times data for diffusion of polymers

If we look at the data in [Table 4.2], this is the trend that we can roughly see. Across the architectures, the diffusion times decrease. Linear chain has the highest values of  $\tau_{diff}$  and then subsequently the values keep on decreasing as we increase complexities in our architectures since the Radius of Gyration (Rg) values also decrease subsequently for their respective architectures. The increase of  $\tau_{diff}$  values across the different cases of number of monomers for a particular architecture is quite obvious. As we increase the number of monomers, the Rg will increase. Thus the polymer will take more time to diffuse a distance of Rg units.



Here as well we do the log-log plot analysis [Figure 4.3] to check the scaling of  $\tau_{diff}$  with respect to the number of monomers ( $N$ ). We have the linear regression for the scatter plot and the slopes of these linear fits give us the scaling exponent for the  $\tau_{diff}$  vs Number of monomers ( $N$ ) for their respective polymer architectures.

Here for all of the architectures, the slopes are  $\approx 2.2$ . Also similar to the scaling analysis data in previous chapters as well, the scaling law doesn't really change much across different polymer architectures. The scaling exponent is mostly around 2.2 under the error limits. So finally the scaling law becomes :

$$\tau_{diff} \approx N^{2.2}$$

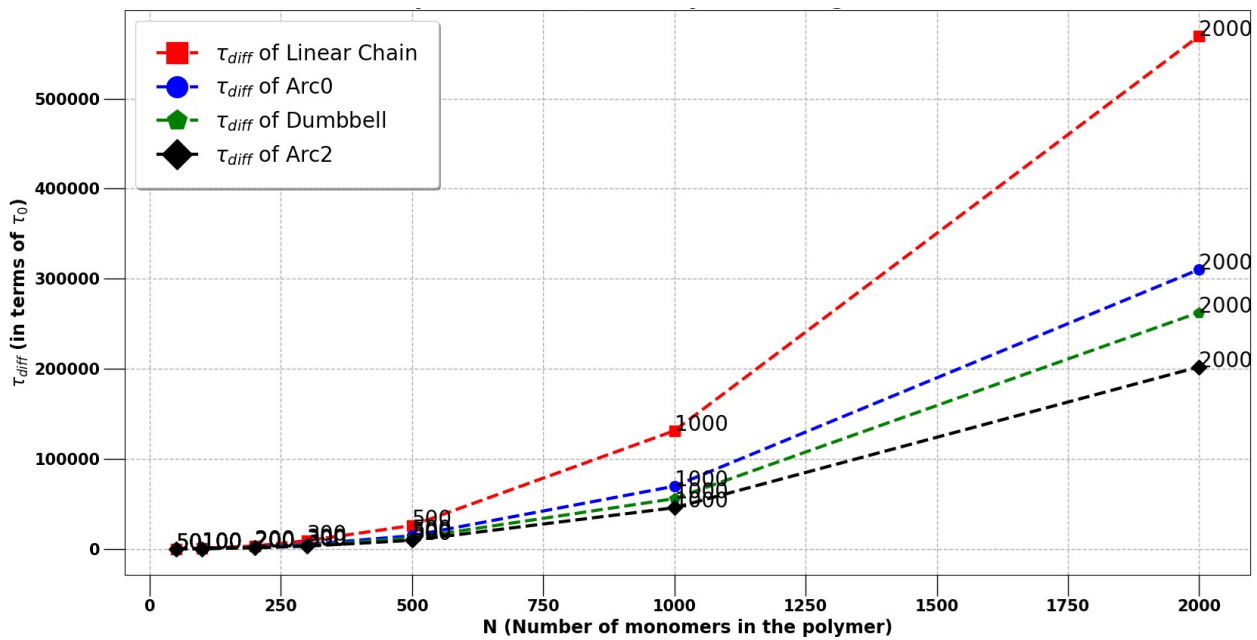


Figure 4.5: Comparison of Diffusion times ( $\tau_{diff}$ ) for Polymer Configurations vs  $N$



# Chapter 5

## Conformation Relaxation

Finally, we discuss about the Conformation Relaxation properties for different polymer architectures. We have different kinds of vectors for all of these different architectures that we have already mentioned in previous chapters. We try to do a detailed analysis for them here.

Although it will be a bit challenging to do comparisons here across the different architectures since all of the vectors across architectures are completely different from each other. Thus there is no direct common ground for comparisons as we had for example in the case of Diffusion where we just had to compare the Centre of Mass related data which is relatively quite straight-forward. Nevertheless, we have tried to form some sort of common ground for comparisons so we try to compare among the slowest relaxation times for each architecture. This means for a particular architecture we see which vector is relaxing the slowest. We choose that vector's relaxation time for comparing  $\tau_{conf}$  for that architecture among other architectures.

### 5.1 Analyzing and choosing the slowest relaxation times across various architectures

Choosing the slowest relaxation times for Linear Chain is relatively straight-forward. We just have to choose the longest possible vector (according to contour length) since it'll take the

longest time to relax. So we can just directly report the values corresponding to the end-to-end vector for Linear Chain’s conformation relaxation times. Even for the Ring polymer it is relatively easy. The longest possible vector can be the diameter. So choose any one diameter and report its relaxation results. We have chosen 4 such diameters just for better averaging but eventually all of them will give similar results after statistically averaging. We can just report the averaged relaxation related results for the Ring polymer’s conformation relaxation times. But things become a bit difficult when we have higher complexity architectures with more cross-links involved.

### 5.1.1 ”Inverted-8(I8)”/Dumbbell Vectors data

For ”Inverted-8”/Dumbbell polymer we have 11 different vectors. Some of them are similar but we will have to individually look at the data for each of them and analyze which one has the slowest relaxation time. We then choose  $\tau_{conf}$  values of that vector for  $\tau_{conf}^{Polymer}$  values of the architecture. We have the data for all of the 11 vectors of the Dumbbell polymer given in [Table 5.1] for vectors 1-8 and in [Table 5.2] for vectors 9-11 :

Table 5.1: ”Inverted-8(I8)”/Dumbbell small loop vectors

<b>N(no.of monomers)</b>	<b>Vec 1</b>	<b>Vec 2</b>	<b>Vec 3</b>	<b>Vec 4</b>	<b>Vec 5</b>	<b>Vec 6</b>	<b>Vec 7</b>	<b>Vec 8</b>
50	143	106	56	134	146	104	53	132
100	583	491	219	491	637	550	221	534
200	2927	1626	821	1851	2789	2868	755	1694
300	5047	2016	1404	2394	5053	3567	1445	2334
500	15094	5977	4063	5571	10867	5261	3908	6399
1000	80827	33510	25055	33590	50147	41369	19068	34150

We can see that the vector 9, 10 and 11 are definitely of the slowest vectors, as expected since they are also the longest vectors as well (contour length wise). They have quite similar relaxation times as well. But one interesting thing to note is that vectors 1 and 5 are also among the slowest vectors as well. In fact their times are also almost similar to vectors 9, 10 and 11. This suggests that for polymer architecture having cross-links, the vector connected to the junction of 1 or multiple cross-links is also the slowest or one of the slowest vectors for the whole polymer. Among the smaller loop also they are the slowest. For example in

Loop A, vector 1 is the slowest then vector 2 and 4 are very similar since they are essentially symmetrical vectors (symmetrical with respect to the cross-link junction point) and vector 3 is the fastest of them all evidently because it is the farthest from the cross-link junction point.

Comparison of  $\tau_{conf}$  for small loop vectors of "Inverted-8(I8)"/Dumbbell polymer :

$$\text{Vec 1} \approx \text{Vec 5} > \text{Vec 2} \approx \text{Vec 4} \approx \text{Vec 6} \approx \text{Vec 8} > \text{Vec 3} \approx \text{Vec 7}$$

Table 5.2: "Inverted-8(I8)"/Dumbbell large (diametric) vectors

<b>N(no.of monomers)</b>	<b>Vec 9</b>	<b>Vec 10</b>	<b>Vec 11</b>
50	140	145	133
100	561	587	562
200	2268	2275	2409
300	4943	4700	5227
500	12202	10270	10903
1000	56147	53528	61428

### 5.1.2 Arc2 Vectors data

For Arc2 polymer we have 15 different vectors. Here as well we will individually look at the data for each of these vectors and analyze which one has the slowest relaxation time. We choose  $\tau_{conf}$  values of that vector for the architecture. The data for all of the 15 vectors of the Arc2 polymer given in [Table 5.3] for vectors 1-8, in [Table 5.4] for vectors 9-12 and in [Table 5.5] for vectors 13-15.

Table 5.3: Arc2 small loop vectors

<b>N(no.of monomers)</b>	<b>Vec 1</b>	<b>Vec 2</b>	<b>Vec 3</b>	<b>Vec 4</b>	<b>Vec 5</b>	<b>Vec 6</b>	<b>Vec 7</b>	<b>Vec 8</b>
50	76	82	120	127	79	51	65	75
100	312	257	158	203	339	255	136	241
200	1415	1336	347	1303	1407	1164	339	1290
300	3145	3298	795	2749	2897	2604	747	1998
500	8675	3455	1726	4633	8664	5654	2588	6610
1000	28282	27651	7317	14420	33493	32706	6504	23673

Here vectors 1-8 follow a similar trend as in the Dumbbell polymer's case :

$$\text{Vec 1} \approx \text{Vec 5} > \text{Vec 2} \approx \text{Vec 4} \approx \text{Vec 6} \approx \text{Vec 8} > \text{Vec 3} \approx \text{Vec 7}$$

Which is justified as well since they are essentially the same 2 small loops connected exactly at one point again. Although much more restricted than the previous architecture's case. But they are symmetric to the cross-link junction point (contour length wise) so a statistically well averaged data of both of them should give quite similar results as well.

Table 5.4: Arc2 large loop vectors

<b>N(no.of monomers)</b>	<b>Vec 9</b>	<b>Vec 10</b>	<b>Vec 11</b>	<b>Vec 12</b>
50	116	93	70	87
100	506	274	203	292
200	1958	1658	984	1421
300	4350	3078	2303	3140
500	11185	7567	4163	6826
1000	78893	44164	33999	66995

Even for the large loop, it behaves exactly in a fashion how small loop vectors behave. The vector connected to the cross-link junction is the slowest then the symmetric vectors being relatively faster than the junction vector but similar to each other and finally the furthest vector from junction being the fastest.

Table 5.5: Arc2 large (diametric) vectors

<b>N(no.of monomers)</b>	<b>Vec 13</b>	<b>Vec 14</b>	<b>Vec 15</b>
50	117	101	63
100	377	405	275
200	1737	1583	1022
300	3577	4015	2353
500	8562	8691	4912
1000	62843	79460	23526

For the "diameter" like vectors, vector 13 and 14 are similar since they are literally symmetric vectors while vector 15 being the fastest since it is the shortest vector connecting the monomer pair of both the small loops. Thus, this result is as expected.

Now the most interesting thing here to note is that Vector 9 is the slowest vector out of every other vectors. This is because it is the largest vector which is directly connected to the junction. We already discussed that the vectors connected to the junctions are among the slowest. Vector 9 belong to the larger loop thus it is the longest such vector. So we choose Vector 9's relaxation time results for comparison of Arc2 across other architectures.

## 5.2 Comparison of $\tau_{conf}$ across various architectures

Now that we have established which vectors and values to choose for comparison of conformation relaxation times across architectures, we have the data given in [Table 5.6] comparing all of them together. The comparison data is slightly indicative of certain things but not completely conclusive enough to claim anything concretely. Some indications are like Linear Chain having the highest conformation relaxation time generally out of all architectures.

N	$\tau_{conf}(LinearChain)$	$\tau_{conf}(Arc0)$	$\tau_{conf}(Dumbbell)$	$\tau_{conf}(Arc2)$
50	231 $\approx 2.31 \cdot 10^2$	120 $\approx 1.20 \cdot 10^2$	140 $\approx 1.40 \cdot 10^2$	116 $\approx 1.16 \cdot 10^2$
100	793 $\approx 7.93 \cdot 10^2$	482 $\approx 4.82 \cdot 10^2$	561 $\approx 5.61 \cdot 10^2$	506 $\approx 5.06 \cdot 10^2$
200	4098 $\approx 4.09 \cdot 10^3$	1555 $\approx 1.55 \cdot 10^3$	2268 $\approx 2.26 \cdot 10^3$	1958 $\approx 1.95 \cdot 10^3$
300	5823 $\approx 5.82 \cdot 10^3$	3604 $\approx 3.60 \cdot 10^3$	4943 $\approx 4.94 \cdot 10^3$	4350 $\approx 4.35 \cdot 10^3$
500	10444 $\approx 1.04 \cdot 10^4$	9631 $\approx 0.96 \cdot 10^4$	12202 $\approx 1.22 \cdot 10^4$	11185 $\approx 1.11 \cdot 10^4$
1000	114410 $\approx 11.44 \cdot 10^4$	58330 $\approx 5.83 \cdot 10^4$	56147 $\approx 5.61 \cdot 10^4$	78893 $\approx 7.88 \cdot 10^4$

Table 5.6: Conformation Relaxation times comparison data

Finally we do the log-log plot analysis [Figure 5.1] in hope of getting any trend for the scaling of  $\tau_{conf}$  with respect to the number of monomers (N). Slopes of the linear fits to our scatter plots should give us the scaling exponent for their respective polymer architectures.

Here for the architectures, the slopes are  $\approx 2.0$  within the error limits. Here we can actually see the slope of the linear fit deviating significantly across the architectures. There does not really seem to be a definite pattern as a consequence of increasing cross-links within the polymer. The scaling exponent is mostly around 2.0 under the error limits. So finally the scaling law somewhat becomes :

$$\tau_{conf} \approx N^2$$



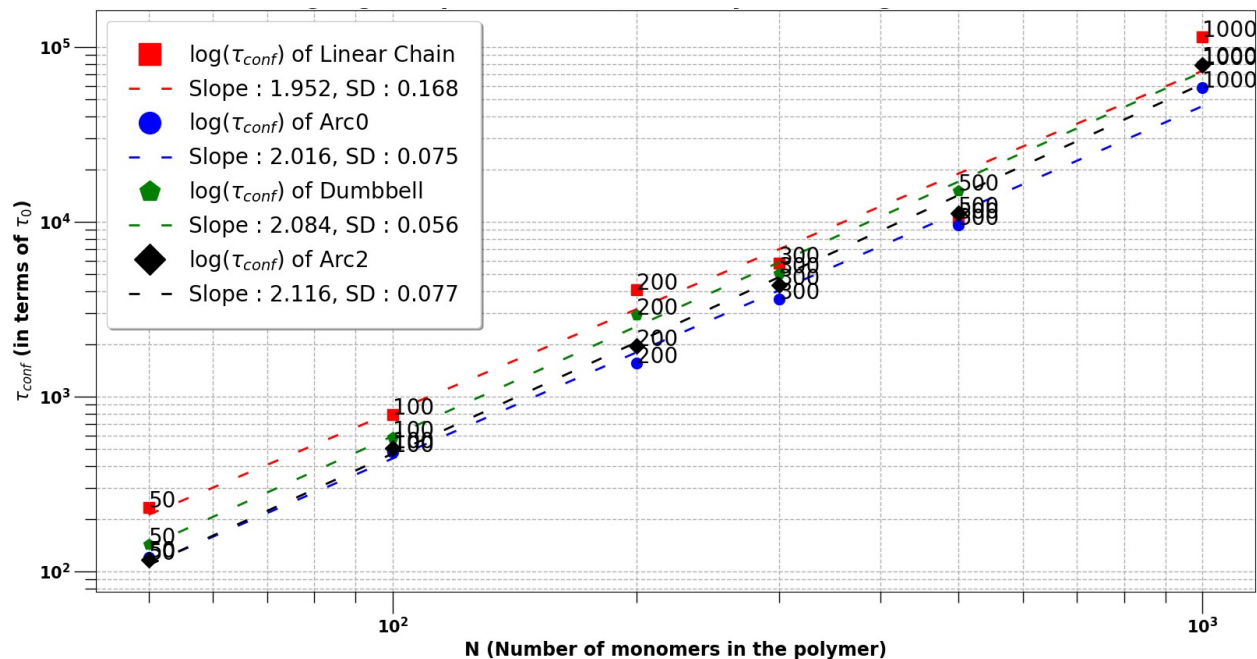


Figure 5.1: log-log Comparison of  $\log(\tau_{conf})$  for Polymer Configurations vs  $\log(N)$

The  $N^2$  scaling pattern can be seen in the comparison plot of Conformation Relaxation times  $\tau_{conf}$  vs Number of Monomers ( $N$ ) in [Figure 5.2]

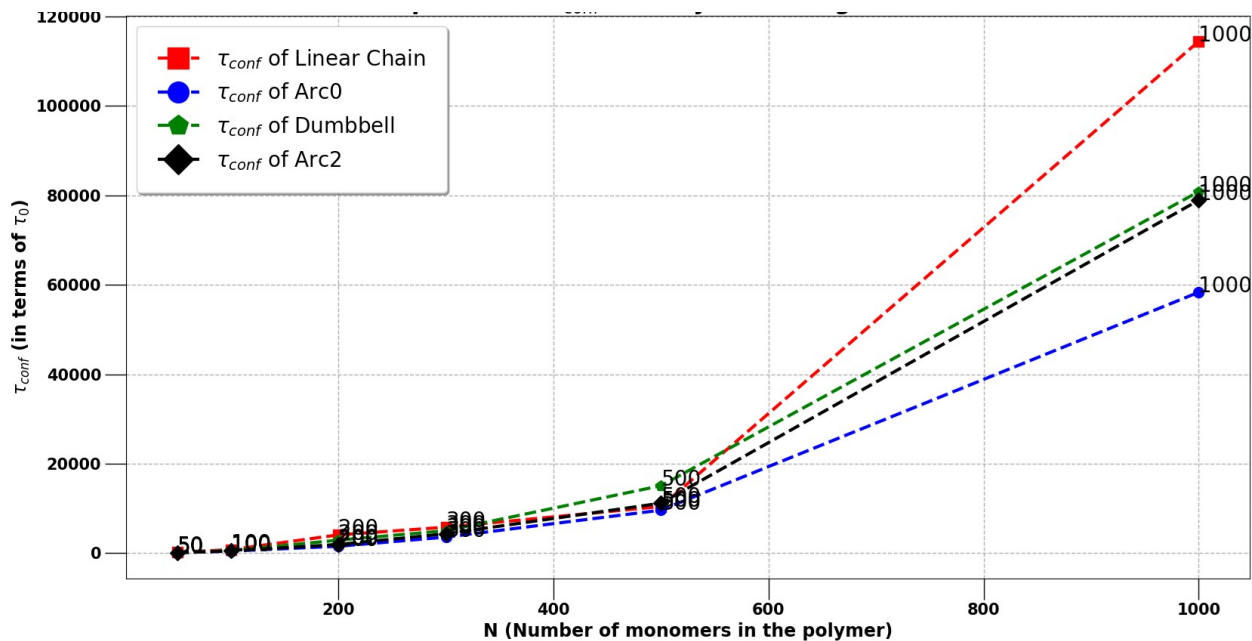


Figure 5.2: Comparison of Conformation Relaxation times ( $\tau_{conf}$ ) for Polymer Configurations vs  $N$



# Chapter 6

## Conclusion and Future Direction

We can see there has been a lot to unpack with just these 4 architectures only. We got some really interesting and fundamental results which actually solidified our understanding of these architectures to an extent while leaving so many more questions as well. We learned and tried different techniques for the analysis some of which we are still testing and trying to extract these results from the perspective of a different technique in hope that it can provide more insights regarding some relatively unclear but exciting results. For example, regarding conformation relaxation times we are trying different analysis techniques like stretched exponential decay analysis rather than the technique mentioned here. The quality of data can also be increased by better averaging especially for conformation relaxation related data.

Our approach has always been to understand the absolute fundamentals first and only then move on to bigger complexities. Thus we replicated and verified the initial data first and then only produced new data regarding further architectures. Having good data for even the static properties like Radius of Gyration ( $R_g$ ) proved to be very beneficial for our dynamics related study since we were able to use that data for our Diffusion related study. Our Diffusion related data is quite concrete and provide a good fundamental base to build upon for further architectures or maybe study of polymers in different confined or melt conditions as well for the future. The Conformation relaxation data still needs some work since we are still figuring out what is the best possible way to extract its meaningful properties. But we have different and exciting ideas to approach it so it should be interesting!

To conclude, the results seem promising and exciting, especially for the architectures.

These results about the Ring, Dumbbell and Arc2 polymers relaxation times call for further investigations of relaxation time changes of topologically modified polymers. Also for future investigation we can study MSD of monomers at different points of chain contour.

This signifies the end of this thesis.

# Bibliography

- [1] M. Doi and S. F. Edwards. *The Theory of Polymer Dynamics*. Oxford University Press, 1988, p. 52.
- [2] M. Doi and S. F. Edwards. *The Theory of Polymer Dynamics*. Oxford University Press, 1988, p. 47.
- [3] M. Doi and S. F. Edwards. *The Theory of Polymer Dynamics*. Oxford University Press, 1988, p. 96.
- [4] Debarshi Mitra, Shreerang Pande, and Apratim Chatterji. “Polymer architecture orchestrates the segregation and spatial organization of replicating E. coli chromosomes in slow growth”. In: *Soft Matter* 18 (30 2022), pp. 5615–5631. DOI: [10.1039/D2SM00734G](https://doi.org/10.1039/D2SM00734G). URL: <http://dx.doi.org/10.1039/D2SM00734G>.
- [5] Debarshi Mitra, Shreerang Pande, and Apratim Chatterji. “Topology-driven spatial organization of ring polymers under confinement”. In: *Phys. Rev. E* 106 (5 Nov. 2022), p. 054502. DOI: [10.1103/PhysRevE.106.054502](https://doi.org/10.1103/PhysRevE.106.054502). URL: <https://link.aps.org/doi/10.1103/PhysRevE.106.054502>.
- [6] Marcus Müller, J. Wittmer, and M. Cates. “Topological effects in ring polymers: A computer simulation study”. In: *Physical review. E, Statistical physics, plasmas, fluids, and related interdisciplinary topics* 53 (May 1998). DOI: [10.1103/PhysRevE.53.5063](https://doi.org/10.1103/PhysRevE.53.5063).
- [7] Michael Rubinstein and Ralph H Colby. *Polymer Physics*. Oxford University Press, 2003, p. 62.
- [8] Michael Rubinstein and Ralph H Colby. *Polymer Physics*. Oxford University Press, 2003, p. 309.